© 2018 IJSRSET | Volume 4 | Issue 4 | Print ISSN: 2395-1990 | Online ISSN : 2394-4099
Themed Section : Engineering and Technology

The spectroscopic (FTIR, FT-Raman, and NMR) analysis, first-order hyperpolarizability, magnetic susceptibility and HOMO–LUMO analysis of 3-(4-Methylphenyl)-2-phenyl-5-(thiophene-2-ylmethylidene)-2, 5-dihydro-1,2,4-triazin-6(1*H*)-one

M. Murali[1], V. Balachandran*[2], B. Narayana[3]

[1]Department of Physics, CARE Group of Institutions, Tiruchirappalli, Tamil Nadu, India

[2]Centre for Research, Department of Physics, A A Government Arts College, Musiri, Tiruchirapalli, Tamil Nadu, India

[3]Department of Studies in Chemistry, Mangalore University, Mangalagangotri, Konaje, Karnataka, India

ABSTRACT

A novel molecule, thiophene derivative 3-(4-Methylphenyl)-2-phenyl-5-(thiophen-2-ylmethylidene)-2,5-dihydro-1,2,4-triazin-6(1*H*)-one has conveniently synthesized and characterized through FT-IR, FT-Raman, NMR spectroscopic studies. Optimized geometrical parameters, like bond lengths and bond angles, and vibrational frequencies have performed with DFT/B3LYP method using 6-31G and 6-311G basis sets using the Gaussian 09W program package. The calculated harmonic vibrational frequencies have been compared with experimental FT-IR and FT- Raman spectra. The observed and calculated frequencies are found to be in good agreement. In addition, Mulliken atomic charges, local reactivity descriptors such as local softness (sk), Fukui function (fk), global electrophilicity and nucleophilicity of the title compound were calculated and discussed. The stability and charge delocalization of the molecule were studied by Natural Bond Orbital (NBO) analysis. The overlapping of atomic orbital along with their predicted energy was explained on the basis of HOMO-LUMO energy gap calculations. Molecular Electrostatic Potential (MEP) map has been studied for predicting the reactive sites. Magnetic susceptibility has been determined for various range of temperature. ^{1}H and ^{13}C Nuclear Magnetic Resonance (NMR) isotropic chemical shifts are evaluated experimentally.

Keywords: FT-IR, FT-Raman, NBO, Mulliken, Fukui Function, NMR, Magnetic Susceptibility

I. INTRODUCTION

Heterocycles are extensively dispersed in nature and participate in major parts of many biochemical processes. Thus, the five-membered aromatic heterocyclic rings are included into new chemical species, by medicinal chemists [1]. Heterocyclic compounds containing thiophene have also received a considerable attention over the past years due to their wide range of biological activity [2]. Thiophene derivatives are important structural fragment in many pharmaceutical and chemical compounds. The thiophene ring is widely found in many varieties of natural products and pharmaceuticals [3] and has functionalized in many domain of research such as electronic devices in solar cells and organic light emitting diode [4, 5]. Molecules containing triazine skeletons show considerable biological and pharmaceutical activities [6, 7].

To the best of our knowledge, the literature survey, 3-(4-Methylphenyl)-2-phenyl-5-(thiophen-2-ylmethylidene)-2,5-dihydro-1,2,4-triazin-6(1*H*)-one has not been carried out with Gaussian 09 package based on DFT using hybrid model B3LYP at 6-31G and 6-311G basis set and hence its molecular analyzation will support the enhancement of new bioactive compounds. Density functional theory (DFT) computations were used for the investigations on charge transfer properties and energy level analyses. The present work involves, vibrational analysis as well as spectroscopic observations in experimentally like FT-IR, FT-Raman, ^{1}H and ^{13}C NMR and also the investigation of the NLO properties were correlated with the theoretical computations carried out with Gaussian 09 package. HOMO-LUMO analysis and molecular electrostatic potential (MEP) were also performed. Interaction between electron donor and acceptor units was understood based on the value of stabilization energy, which was obtained using natural bonding orbital (NBO) theory. Magnetic susceptibility of the title molecule was calculated and analyzed by using the graphical representation of $1/\chi$ versus Temperature.

II. EXPERIMENTAL DETAILS

A mixture of 2-(4-methylphenyl)-4-(thiophen-2-ylmethylidene)-1,3-oxazol-5(4*H*)-one (2.69g, 0.01 mol), and phenyl hydrazine (1.08g, 0.01mol) in 30ml glacial acetic acid were heated under reflux for 2-3 h. The reaction mixture was cooled and poured on cold water, the solid mass obtained was filtered off, washed with cold water, and recrystallized from methanol and Dimethyl formamide 1:1 mixture. Single crystals were grown from methanol: Di methyl formamide (1:1) mixture by the slow evaporation method (M.P. 459K-460K). The molecular structure of the 3-(4-Methylphenyl)-2-phenyl-5-(thiophen-2-ylmethylidene)-2,5-dihydro-1,2,4-triazin-6(1*H*)-one is shown in Fig. 1.

The FTIR spectrum of the 3-(4-Methylphenyl)-2-phenyl-5-(thiophen-2-ylmethylidene)-2,5-dihydro-1,2,4-triazin-6(1*H*)-one molecule has been recorded using Perkin-Elmer spectrum RX1 spectrophotometer with composition of the pellet at room temperature in the region 4000-400 cm^{-1} with optical resolution of 0.4 cm^{-1}. The FT-Raman spectrum was also recorded by BRUKER-RFS 27 spectrometer consisted of a quartz beam splitter with high sensitive Ge diode detector, to measure spectral measurements. For the excitation of the spectrum in the emission of Nd:YAG laser was used and the excitation wavelength was 1064 nm, maximum power was 100 mW was carried out on the sample. Nuclear magnetic resonance (^{1}H and ^{13}C NMR) spectra were recorded on Bruker 300 AVANCE spectrometer at 300MHz for ^{1}H and 75 MHz for ^{13}C using chloroform ($CDCl_3$) as solvent; the chemical shifts are expressed in the form of ppm using tetramethylsilane (TMS) as internal standard.

III. COMPUTATIONAL DETAILS

The DFT calculations of the title compound were carried out using Gaussian 09 software [8] by applying Becke's three parameter hybrid model with the Lee-Yang-Parr correlation functional (B3LYP) method. The 6-31G and 6-311G basis sets were employed to predict the optimized molecular structure (Fig. 1) and vibrational numbers [9,10] and a scaling factor (0.9613 and 0.9837) must be used for attaining a significantly better agreement with experimental data [11] and no imaginary wavenumber modes were obtained. This implies that a true minimum on the potential surface. Then frequency calculations were employed to confirm the structure as minimum points in energy. The observed dissimilarity between theory and experiment could be a significance of the anharmonicity and the general propensity of the quantum chemical methods to overvalue the force constants at the exact equilibrium geometry. The optimized geometrical parameters of the title molecule (B3LYP/6-31G and B3LYP/6-311G) are given in the Table 1 Molecular electrostatic potential (MEP) plot has been presented to know about the different sites of electrophilic and nucleophilic attacks of the compound. The chemical reactivity behavior of the compound was predicted based on reactivity indices obtained by HOMO and LUMO energy eigen values.

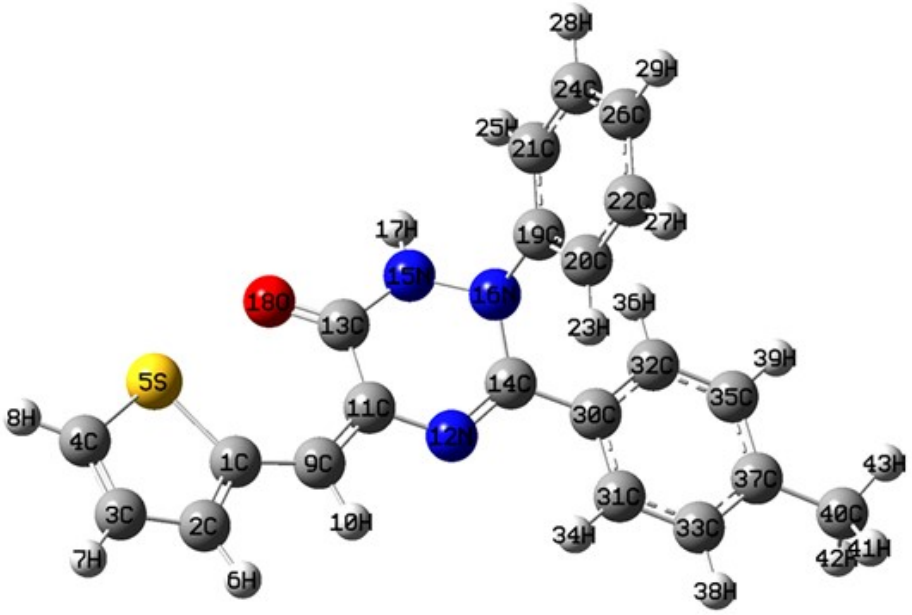

Figure 1. Optimized geometrical structure and atom numbering of 3-(4-Methylphenyl)-2-phenyl-5-(thiophen-2-ylmethylidene)-2, 5-dihydro-1, 2, 4-triazin-6(1*H*)-one

Table 1. Optimized structural parameters of 3-(4-Methylphenyl)-2-phenyl-5-(thiophen-2-ylmethylidene)-2,5-dihydro-1,2,4-triazin-6(1*H*)-one utilizing B3LYP/6-31G and 6-311G density functional calculation

Parameter	Bond Length (A°)		Parameter	Bond Length (A°)		Parameter	Bond Angle (A°)		Parameter	Bond Angle (A°)		Parameter	Bond Angle (A°)	
	B3LYP/ 6-31G	B3LYP/ 6-311G		B3LYP/ 6-31G	B3LYP/ 6-311G		B3LYP/ 6-31G	B3LYP/ 6-311G		B3LYP/ 6-31G	B3LYP/ 6-311G		B3LYP/ 6-31G	B3LYP/ 6-311G
C1-C2	1.39	1.39	C19-C20	1.40	1.40	C2-C1-S5	109.45	109.40	C11-C13-O18	125.63	125.55	C20-C22-H27	119.26	119.22
C1-S5	1.83	1.83	C19-C21	1.40	1.40	C2-C1-C9	122.19	122.44	N15-C13-O18	120.11	120.11	C26-C22-H27	120.11	120.13
C1-C9	1.43	1.43	C20-C22	1.40	1.40	S5-C1-C9	128.36	128.16	N12-C14-N16	121.23	120.89	C21-C24-C26	120.40	120.46
C2-C3	1.42	1.42	C20-H23	1.08	1.08	C1-C2-C3	115.26	115.36	N12-C14-C30	120.55	120.84	C21-C24-H28	119.45	119.39
C2-H6	1.08	1.08	C21-C24	1.40	1.39	C1-C2-H6	121.36	121.35	N16-C14-C30	118.21	118.25	C26-C24-H28	120.15	120.15
C3-C4	1.37	1.37	C21-H25	1.08	1.08	C3-C2-H6	123.37	123.29	C13-N15-N16	123.21	122.79	C22-C26-C24	119.41	119.33
C3-H7	1.08	1.08	C22-C26	1.40	1.40	C2-C3-C4	113.04	113.17	C13-N15-H17	118.86	118.61	C22-C26-H29	120.31	120.35
C4-S5	1.79	1.79	C22-H27	1.09	1.08	C2-C3-H7	123.50	123.50	N16-N15-H17	117.36	117.42	C24-C26-H29	120.28	120.32
C4-H8	1.08	1.08	C24-C26	1.40	1.40	C4-C3-H7	123.46	123.33	C14-N16-N15	112.72	112.75	C14-C30-C31	119.51	119.75
C9-H10	1.09	1.09	C24-H28	1.09	1.08	C3-C4-S5	112.65	112.61	C14-N16-C19	121.86	122.03	C14-C30-C32	121.83	121.67
C9-C11	1.37	1.37	C26-H29	1.08	1.08	C3-C4-H8	128.36	128.51	N15-N16-C19	116.03	116.30	C31-C30-C32	118.63	118.56
C11-N12	1.41	1.42	C30-C31	1.41	1.41	S5-C4-H8	118.99	118.87	N16-C19-C20	121.29	121.23	C30-C31-C33	120.51	120.54
C11-C13	1.48	1.48	C30-C32	1.41	1.40	C1-S5-C4	89.60	89.45	N16-C19-C21	119.08	119.28	C30-C31-H34	118.52	118.55
N12-C14	1.30	1.30	C31-C33	1.39	1.39	C1-C9-H10	112.27	112.30	C20-C19-C21	119.63	119.49	C33-C31-H34	120.96	120.91
C13-N15	1.38	1.38	C31-H34	1.08	1.08	C1-C9-C11	135.68	135.63	C19-C20-C22	119.84	119.94	C30-C32-C35	120.45	120.49
C13-O18	1.25	1.25	C32-C35	1.40	1.39	H10-C9-C11	112.01	112.04	C19-C20-H23	120.13	120.19	C30-C32-H36	119.64	119.62
C14-N16	1.43	1.43	C32-H36	1.08	1.08	C9-C11-N12	116.19	116.33	C22-C20-H23	120.02	119.87	C35-C32-H36	119.91	119.89
C14-C30	1.47	1.47	C33-C37	1.41	1.41	C9-C11-C13	126.12	126.25	C19-C21-C24	120.10	120.14	C31-C33-C37	121.17	121.21
N15-N16	1.42	1.42	C33-H38	1.09	1.08	N12-C11-C13	117.48	117.19	C19-C21-H25	120.15	120.22	C31-C33-H38	119.47	119.42
N15-H17	1.01	1.01	C35-C37	1.40	1.40	C11-N12-C14	121.40	121.14	C24-C21-H25	119.75	119.64	C37-C33-H38	119.36	119.37
N16-C19	1.44	1.44	C35-H39	1.09	1.08	C11-C13-N15	113.94	113.99	C20-C22-C26	120.61	120.64	C32-C35-C37	121.21	121.24

IV. Result and Discussion

A. Molecular geometry

The optimized geometrical parameters, like bond length and bond angles calculated by B3LYP/6-31G and B3LYP/6-311G method are depicted in the Table 1 with atom numbering arrangement is given in Fig. 1. From the Table 1 it is showed that the optimized structure yields identical bond lengths for the C–C bonds on the benzene ring at the B3LYP/6-311G level. The magnitudes of the C_1-C_2 and C_2-C_3 bonds are found to be 1.39 Å and 1.42 Å at B3LYP/6-311G level respectively. They are larger than C=C bond length (1.34 Å) but shorter than that of the single bond C-C bond length (1.54 Å) [12]. For the C-S bond, carbon sulfur bond length is calculated at B3LYP/6-311G level is 1.79 Å which is smaller than the bond length of the single C-S bond (1.82 Å). The bond lengths of C_{11}—N_{12} and N_{12}—C_{14} are 1.42 Å and 1.30 Å at B3LYP/6-311G level respectively. They are much shorter than the normal C-N bond length (1.47 Å) and the C=N bond length (1.33 Å) [13].

The bond angles C_2—C_3—H_7 and C_4—C_3—H_7 are 123.5° and 123.46° at B3LYP/6-311G level respectively. This implies that the C_3—H_7 bond is symmetrically disposed on C_3 atom. Similarly, the bond angles of C_{19}—C_{20}—H_{23} and C_{22}—C_{20}—H_{23} are 120.13° and 120.02° respectively, which indicate that C_{20}—H_{23} is symmetrical disposed on C_{20} atom. In the title compound, the bond angles are C_9—C_{11}—C_{13}→126.25°, S_5—C_1—C_9→128.16° and C_1—C_9—C_{11}→ 135.63° calculated at B3LYP/6-311G level.

B. Vibrational analysis

The observed and calculated FTIR and FT-Raman spectra of 2-(4-methylphenyl)-4-(thiophen-2-ylmethylidene)-1,3-oxazol-5(4*H*)-one are shown in Figs. 2 and 3 respectively. The observed FTIR and FT-Raman wavenumbers along with the theoretical IR and Raman wavenumbers along with their relative intensities and possible assignments are summarized in

C-S, C-N, C-H vibrations

The assignment of the C-S stretching vibration in different compounds is difficult. The C-S stretching modes at 672 cm^{-1} in the IR spectrum and theoretically at 696 and 671 cm^{-1} reported by Kaur et al. [14]. The C—S stretching mode is reported at about 640 cm^{-1} by Cravino et al. [15]. The band observed at 685 cm^{-1} in the IR spectrum of the title compound and 669, 667 cm^{-1} calculated from DFT are assigned as the C–S stretching modes. The identification of C—N vibrations is a very difficult task, meanwhile the mixing of vibrations is possible in this region. Silverstein et al., [16] assigned C—N stretching absorption in the region 1266-1382 cm^{-1} for aromatic amines. In 1,2,4-triazole the band observed at 1390 and 1327 cm^{-1} are assigned to C-N stretching [17]. For the title compound the C—N stretching mode is observed at 1527 cm^{-1} in the IR spectrum, 1526 cm^{-1} in the Raman spectrum and theoretically 1526 cm^{-1} for B3LYP/6-311G. Aromatic compounds commonly exhibit multiple weak bands in the region of 3100-3000 cm^{-1} due to the aromatic C—H stretching vibrations. They are not appreciably affected by the nature of the substituent [18, 19]. In the present study, the C—H stretching vibrations of the title compound are observed at 3101, 3061 and 2980 cm^{-1} in the FT-IR spectrum and the same type of vibrations are observed at 3101 and 3052 cm^{-1} in the FT-Raman spectrum. The C-H in-plane bending vibrations usually obtained in the region 1390-990 cm^{-1} and is very useful characterization purpose [20]. The calculated frequencies 1155, 1146 and 1084 cm^{-1} at B3LYP/6-311G are assigned to C—H in-plane bending vibration which showed excellent agreement with observed C—H in-plane bending vibration of IR spectra for the title compound at 1148 cm^{-1} and Raman spectra 1157 and 1085 cm^{-1}. The C—H out-of-plane bending deformation is usually between 1000-700 cm^{-1} [21]. The C—H out of plane modes are observed at 973, 919, 865, 824 cm^{-1} in the IR spectrum and band observed at 820 cm^{-1} in the FT-Raman spectrum of the title compound. This also shows good agreement with theoretically scaled harmonic wavenumber values.

N-H, N-N vibrations

In the literature, some N-H stretching modes observed for the different substituent-triazole ring are 3383 cm^{-1} [22], 3470 cm^{-1} [23] and 3417 cm^{-1} [24] as experimental. As can be

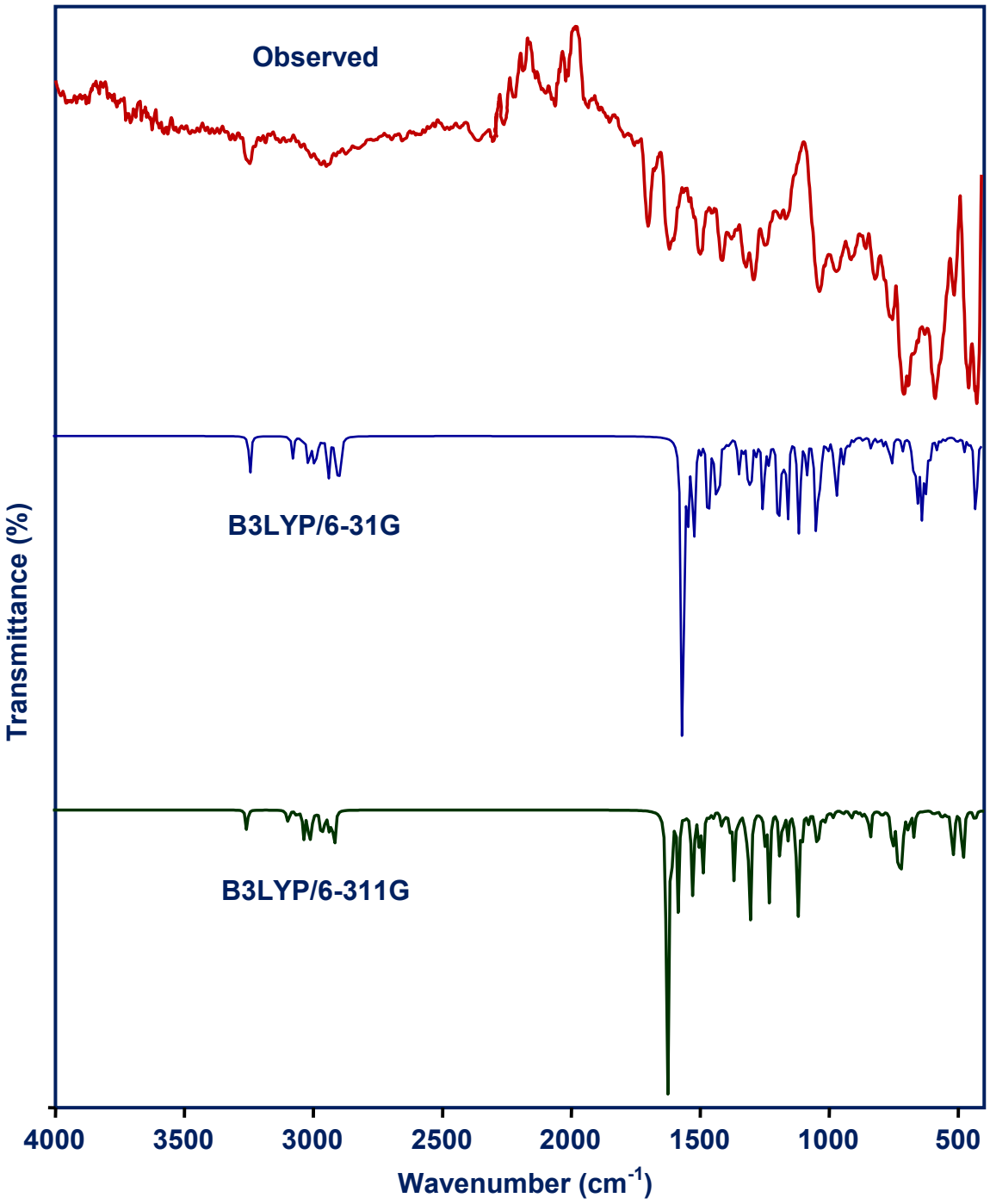

Fig. 2 Observed and simulated infrared spectra of 3-(4-Methylphenyl)-2-phenyl-5-(thiophen-2-ylmethylidene)-2, 5-dihydro-1, 2, 4-triazin-6(1*H*)-one

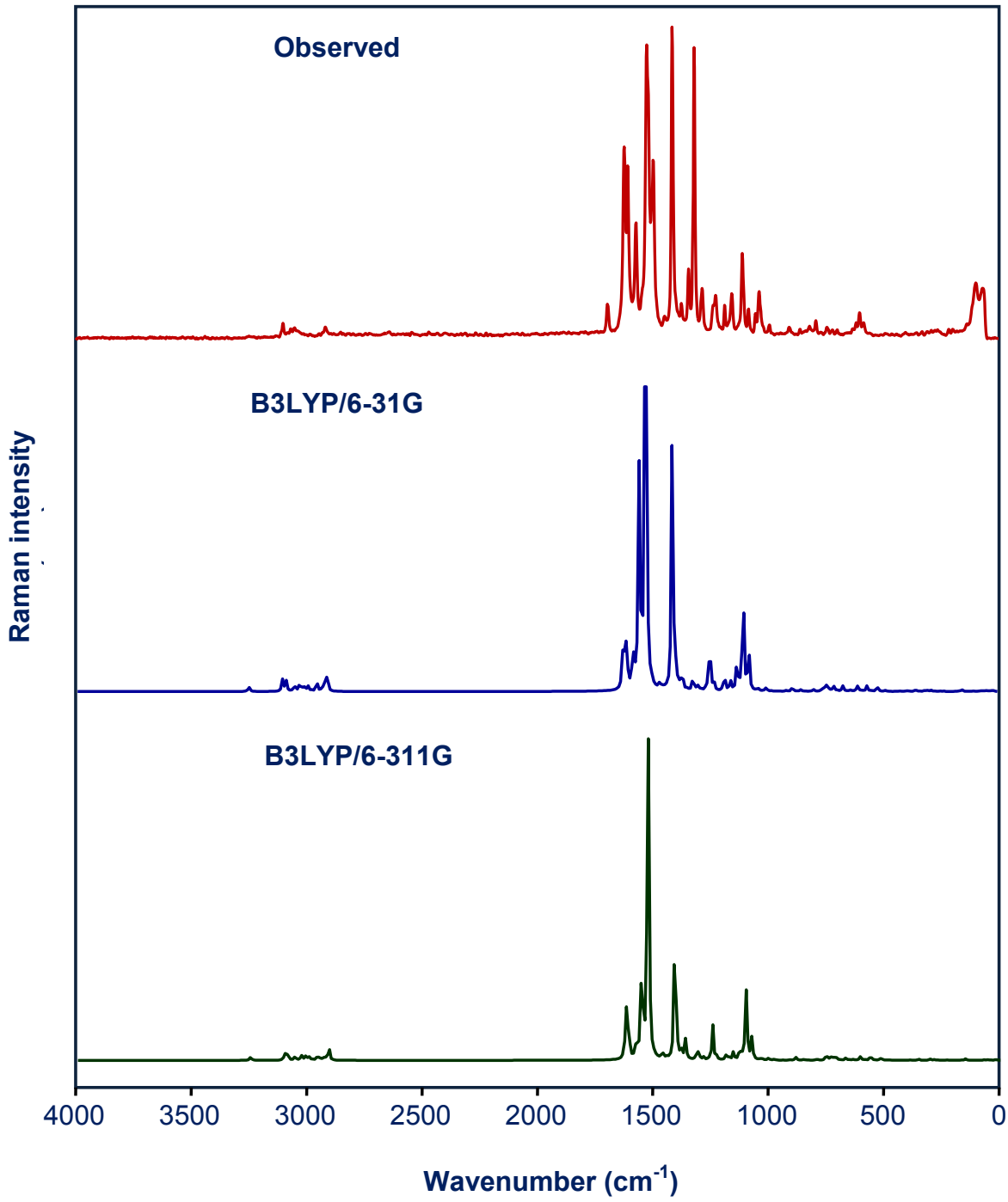

Fig. 3 Observed and simulated Raman spectra of 3-(4-Methylphenyl)-2-phenyl-5-(thiophen-2-ylmethylidene)-2, 5-dihydro-1, 2, 4-triazin-6(1*H*)-one

Table 2. Experimental and Calculated B3LYP/ 6-31G and B3LYP/ 6-311G levels of vibrational frequencies (cm^{-1}), of 3-(4-Methylphenyl)-2-phenyl-5-(thiophen-2-ylmethylidene)-2,5-dihydro-1,2,4-triazin-6(1*H*)-one

S.No.	Observed frequency (cm^{-1})		Calculated frequency (cm^{-1})				Vibrational assignment/ (%)
	FT-IR	FT-Raman	Unscaled		Scaled		
			B3LYP/ 6-31G	B3LYP/ 6-311G	B3LYP/ 6-31G	B3LYP/ 6-311G	
1.	3250	3246	3639	3611	3254	3250	νNH(99)
2.	3101	3101	3293	3259	3107	3102	νCH(97)
3.			3244	3211	3092	3089	νCH(98)
4.	3061		3239	3211	3063	3060	νCH(98)
5.		3052	3238	3208	3055	3051	νCH(97)
6.			3233	3202	3038	3032	νCH(98)
7.			3228	3201	3032	3029	νCH(98)
8.	2980		3225	3193	3016	3013	νCH(99)
9.			3217	3191	3008	3006	νCH(97)
10.			3205	3177	2996	2995	νCH(97)
11.			3197	3169	2983	2982	νCH(98)
12.			3195	3166	2960	2961	νCH(98)
13.			3192	3162	2956	2952	νCH(97)
14.			3165	3138	2938	2939	νCH(98)
15.			3130	3097	2930	2931	$\nu_{ass}CH_3$(98)
16.		2918	3098	3065	2924	2920	$\nu_{ass}CH_3$(99)
17.	2912		3038	3013	2913	2910	$\nu_{ss}CH_3$(98)
18.		1623	1698	1673	1625	1622	νCC(68), νCO(18), νCN(12)
19.	1614		1671	1652	1614	1615	δring(58), νCN(22)
20.		1608	1660	1639	1603	1606	νCO(57), νCC(18), δring(12), νCN(10)
21.	1581		1657	1630	1583	1580	δring(69), νCO(21), νCC(15)
22.		1573	1644	1625	1576	1573	δring(59), νCC(21), νCN(16)
23.	1554		1626	1608	1555	1553	δring(60), νCN(24), $\delta_{rock}CH_3$(12)
24.	1527	1526	1603	1582	1528	1526	νCN(57), δring(22), νCC(14)
25.			1573	1557	1519	1518	νCC(66), δring(18)
26.	1492	1498	1567	1551	1502	1499	δring(55), νCC(23), νCN(12)
27.			1553	1542	1488	1485	δring(54), νNH(20)
28.			1536	1531	1465	1463	νCH_3(61), δring(19)
29.	1445		1533	1530	1449	1446	νCH_3(58), δring(19)
30.		1415	1514	1503	1419	1415	δring(54), δring(21), νCH(11)
31.	1408		1493	1473	1411	1409	δring(53), νCC(21), νCN(12)
32.			1465	1456	1396	1395	δCH_3(54), δring(18), νCN(10)
33.			1462	1451	1385	1382	δring(58), δCH_3(20), νCC(12)
34.		1375	1452	1443	1380	1377	νNH(57), δring(18), νCO(10)
35.	1364		1439	1429	1368	1363	δring(58), νCC(16), νCN(12)
36.		1345	1397	1393	1346	1345	δ_{rock}ring(54), νCN(18), νNN(12)
37.		1321	1384	1368	1322	1320	δ_{rock}ring(55), νCC(18), δring(10)
38.	1310		1378	1367	1316	1311	δ_{rock}ring(48), δCH_3(15)
39.			1368	1348	1302	1300	δring(49), δring(18), νCN(10)
40.	1286	1287	1367	1339	1288	1285	δring(48), δring(22), νNN(12)
41.			1358	1337	1264	1263	νCN(55), νCC(20), δring(11)
42.	1243		1327	1314	1248	1245	νCN(55), δCH(21), νNH(10)
43.		1227	1287	1277	1230	1228	δring(54), ν_{ass}NH(18)
44.			1275	1262	1121	1118	δring(59), νCN(18), δCC(11)
45.			1257	1246	1106	1102	δring(57), νCC(18), δCN(10)
46.		1188	1251	1236	1189	1188	δring(54), νCN(13), νCC(10)
47.	1175		1240	1230	1181	1176	δring(55), δCH(15), δCN(12)
48.		1157	1237	1226	1158	1155	δCH(57), δring(16), νCC(10)
49.	1148		1224	1213	1145	1146	δCH(49), νCC(12)
50.			1217	1209	1130	1128	δring(48), δ_{rock}CH(21), δCH(10)
51.		1111	1171	1161	1114	1110	δring(47), νNN(18), δCH_3(12)
52.			1142	1132	1102	1099	νCN(48), νNN(16), δring(12)
53.		1085	1134	1121	1085	1084	δCH(47), δring(18), νCN(11)
54.		1078	1120	1110	1078	1075	νNN(50), δring(21), δCN(10)
55.		1055	1099	1094	1055	1053	γCC(52), $\delta_{rock}CH_3$(17), δCH(12)
56.			1096	1084	1053	1048	δCH(52), νCC(18), νCN(11)
57.		1039	1072	1062	1044	1040	δring(51), νCN(18), νNN(10)
58.	1029		1061	1052	1036	1031	δring(52), νCC(19), νNN(10)
59.			1053	1048	1018	1015	δring(54), δCC(22), νNC(13)
60.			1036	1030	1005	1002	δring(48), δCH_3(21), δCH(11)
61.		995	1032	1024	999	996	$\delta_{rock}CH_3$(47), δring(22), νNN(10)
62.			1027	1023	985	982	γCH(49), γCC(13)
63.	973		1017	1017	978	975	γCH(48), γCC(13), δCH_3(10)
64.			1005	1005	945	943	γCH(49), γCC(13)
65.	919		993	997	925	921	γCH(48), γCC(12)

66.		910	982	976	914	911	δring(54), γCH(16), νCN(10)
67.			973	967	889	885	γCH(49), γCC(18), δring(10)
68.			952	951	883	879	γCH(48), γCC(18), γCN(11)
69.	865		937	937	868	866	γCH(44), γCC(16), γCN(10)
70.			881	877	853	851	γCH(43), γCC(17), γCN(11)
71.			872	867	850	845	δring(44), δCC(19), δCH(11)
72.			869	866	839	838	γCH(45), γCC(19), δCH_3(10)
73.	824	820	864	865	826	825	γCH(48), γCC(13)
74.			860	858	810	807	γCH(44), γCC(16), δ_{rock}CH(10)
75.		793	834	828	796	792	δring(47), δring(18), δCN(11)
76.	757		815	808	759	755	δring(47), δring(17), δCC(10)
77.			796	793	752	750	γCH(44), γCC(13), γNN(10)
78.		745	784	779	745	746	τCC(42), γCH(12), γNN(10)
79.			769	767	739	733	γCH(43), γCC(12), γCN(11)
80.			742	736	729	726	δring(43), τCC(13), δCN(10)
81.			738	730	722	720	δ_{wag}CH(42), νCC(12), νCN(11)
82.			731	727	710	712	γCH(43), δCN(12), δCS(10)
83.	702		721	717	705	704	δring(42), δNN(11), νCO(10)
84.			719	716	694	689	γCH(43), γCC(12), νCN(10)
85.	685		711	699	669	667	νCS(42), γCH(11), γCC(10)
86.			676	672	654	650	δring(41), δCS(12), νNN(10)
87.	635		666	659	638	635	δring(42), γCN(13), δCS(11)
88.			649	649	625	624	δring(40), δCC(13)
89.		603	621	610	606	605	δCS(41), δNH(13), δCN(10)
90.			602	599	592	592	γCH(40), γCC(12), γNH(10)
91.	580		601	594	583	581	γCH(42), γCC(12), γCS(10)
92.			574	571	564	560	δNC(43), δring(11), δCS(11)
93.			561	559	545	543	δring(41), δNC(12), δCC(11)
94.			534	529	521	519	γNH(40), γCH(12), δCC(10)
95.	514		522	518	516	512	δring(42), γCH(11), γCS(10)
96.			519	511	495	492	γCH(41), δring(12), τCH(10)
97.			506	502	482	479	γNH(41), γCH(12), γCC(10)
98.			467	467	434	432	δCO(40), δring(12), δNN(11)
99.			431	430	417	416	γCH(41), γCC(11), δCC(10)
100.			427	426	396	392	γCH(39), γCC(13), γCN(11)
101.			413	409	385	385	δring(39), γNN(14), δCO(10)
102.			394	393	352	351	γNH(38), γNN(13), δring(11)
103.			378	379	335	334	γNH(38), δring(14), δCC(10)
104.			359	358	314	309	δCH_3(38), δring(13), γNN(11)
105.			346	345	303	299	δring(37), γCO(13), γCH(10)
106.			300	302	285	282	γCH_3(38), γNN(14), γCH(10)
107.			282	285	266	265	δring(37), γCN(11), γNN(11)
108.		266	273	271	244	241	δring(38), δCH_3(11)
109.			255	253	229	228	δring(37), δCO(12), δNH(10)
110.			199	198	180	179	δring(36), δCO(11), δCS(10)
111.			185	185	165	162	δring(37), δCC(11), δCN(10)
112.			180	177	151	149	δNN(37), δring(10)
113.			141	140	125	121	δring(38), δCO(11), δCS(10)
114.			132	133	119	114	γCH_3(39), δring(11)
115.		101	102	102	100	98	δring(38), γCO(12), γCS(11)
116.		73	74	74	72	70	γCO(37), γCS(13), γCC(10)
117.			60	59	59	55	δring(39), γCO(12), γCS(10)
118.			54	56	55	52	τring(38), γCH(13), γCC(11)
119.			46	46	44	43	δring(39)
120.			39	40	36	38	δring(39), γCH_3(11)
121.			35	39	33	33	γCH_3(38), γCH(11)
122.			23	27	22	20	δring(38), γCH_3(10)
123.			10	14	10	10	δring(39)

seen in the Table 2. The N—H stretching mode was observed at 3250 cm^{-1} in the FT-IR spectrum and at 3246 cm^{-1} in the FT- Raman spectrum. At the same time, the calculated N—H stretching mode as 3254 cm^{-1} for B3LYP/6-31G and 3250 cm^{-1} for B3LYP/6-311G. These difference between the experimental and calculated values for N—H stretching vibrations can explained by the existence of the N-H…O strong intermolecular hydrogen bonds [22, 25]. The N—N stretching is expected in the range 1200-950 cm^{-1} [26]. The DFT computation

for the title compound gives mode arising from the calculated N—N stretching at 1075 cm^{-1} corresponding to the peak at 1078 cm^{-1} in the Raman spectrum. The N—N stretching mode has been reported at 1134 cm^{-1} (IR), 1138 cm^{-1} (Raman) 1136 cm^{-1} (DFT) by Panicker er al. [27], at 1124 cm^{-1} by Binil et al. [28] and 1132 (IR), 1139 (DFT) cm^{-1} by Mangalam et al. [29].

C=O vibrations

The carbonyl group is contained in a large number of different classes of compounds, for which a strong absorption band due to C=O stretching vibration is observed in the range of 1850-1550 cm^{-1} [30]. This region is considered as a very important region by organic chemists. The carbonyl groups in the triazine fragment give rise to bands in the region of 1720-1790 cm^{-1} [31]. The carbon oxygen double bond is formed by π - π between carbon and oxygen, and the lone pair of electron on oxygen also determines the nature of the carbonyl group. For the title compound, the C=O stretching bands are observed at 1608 cm^{-1} in the Raman spectrum and at 1603, 1606 cm^{-1} theoretically by B3LYP/6-31G and B3LYP/6-311G, respectively. The position of the peak or the band not only tells the presence of a group but also reveals a good deal about the environments affecting the group [32]. The wavenumber due to C=O stretch mainly depends on the bond strength which in turn depends upon inductive, conjugative, field and steric effects.

CH_3 modes

The CH_3 stretching vibrations occurs at lower frequencies expected in the range (2900-3050 cm^{-1}) [21, 33] and for the title compound, the asymmetric stretching mode of the methyl group are calculated to be at 2931 and 2920 cm^{-1} and the symmetric mode is 2910 cm^{-1}. The band observed at 2918 cm^{-1} in the Raman spectrum was assigned asymmetric stretching mode of the methyl group of the title compound. The asymmetric and symmetric bending vibrations of the methyl group normally appear in the region of 1400-1485 cm^{-1} and 1380-1420 cm^{-1} [30]. The bending vibrations calculated as 1396 and 1395 cm^{-1} by B3LYP/6-31G and B3LYP/6-311G, respectively were assigned as CH_3 bending modes. The calculated vibrations are assigned as the C–H stretching vibration of methyl group which is in good agreement with the experimental work.

Thiophene ring vibrations

The thiophene ring is essentially formed by three groups S—C, C=C and C—H which their stretching vibration modes are arising in three different regions of spectra. In general, the assignment of band due to the C—S stretching vibration in different compounds is difficult in the infrared. The absorption of this group is of variable intensity and may be found over a wide region 1035-245 cm^{-1} both in aliphatic and aromatic sulfides [34]. The C-S stretching vibration results in strong bands in Raman spectra which are normally easy to identify [35-38]. The computed C–S stretching vibrational mode at 669 cm^{-1} for B3LYP/6-31G and 667 cm^{-1} for B3LYP/6-311G. The C—S group is less polar than the carbonyl links and has a considerably weaker band in the infrared. In consequence, the band is not intense, and it falls at lower frequencies, where it is much more susceptible to coupling effects and identification is therefore difficult and uncertain. The in-plane and out-of-plane bending vibrations of C—S group were also found well within the characteristic region and in line with the observed frequencies. The in-plane bending vibrational mode of C—S is assigned at 603 cm^{-1} for Raman spectrum and 605 cm^{-1} for calculated value in B3LYP/6-311G.

C. Frontier molecular orbital

Frontier molecular orbitals (FMOs) are the highest occupied molecular orbital (HOMO) and the lowest unoccupied molecular orbital (LUMO). The energies as well as the energy gap of these molecular orbitals, have many applications in physics, chemistry and biology. The electronic structure of the molecule, charge transport properties and optical properties of the molecule are mainly depending on the energy difference of HOMO and LUMO; hence, it is essential to determine the HOMO-LUMO energy gap [39].

The small orbital gap in a molecule is represented more polarizable and it is generally associated with a high chemical reactivity, low kinetic stability and is also termed as soft molecule [40]. The HOMO-LUMO energy separation has been used as a simple indicator of kinetic stability [41]. The electron affinity (A) and ionization potential (I) are used to estimate the energy barrier of the electrons. The electronegativity (χ) and hardness (η) calculation are all based on the commonly used finite difference approximation, leading to $\chi = (I/A)/2$ and $\eta = (I-A)$ [42]. The hardness is associated with the stability of the chemical system and it corresponds to the gap between the HOMO and LUMO energies. The larger

the HOMO-LUMO gap, the harder the molecule. Generally hard nucleophiles are having a low HOMO energy, soft nucleophiles are having a high HOMO energy, hard electrophiles are having a high LUMO energy and soft electrophiles are having a low LUMO energy. Parr et al. [43] have proposed electrophilicity index as a measure of energy lowering due to maximal electron flow between donor and acceptor. They defined electrophilicity index (ω) as $\omega = \mu^2/2\eta$, where μ is the chemical potential. When two molecules react, the one that acts as an electrophile has a higher electrophilicity index and nucleophile has a lower electrophilicity index. This index evaluates the stabilization in energy when the system obtains an additional electronic charge from environment [44]. Increase the HOMO-LUMO energy gap decreases reactivity of the compound that leads to increase the stability of the compound. The energies of HOMO and LUMO are negative, which indicates that the title compound is stable. DFT based descriptors have helped in many ways to understand the structure of the molecules and their reactivity by calculating the chemical potential, global hardness and electrophilicity. The total electronic densities of states (DOSs) of the title compound was computed and calculated energy gap clearly as shown in Fig. 4

From the Fig.5 the energy values of HOMO and LUMO for the title compound, E_{HOMO} = -5.26043 eV and E_{LUMO} = -2.05688 eV. The HOMO-LUMO energy gap of the studied compound, ΔE = 3.20355 eV that indicates the chemical reactivity of the molecule. The ionization energy(I) and electron affinity(A) by using HOMO and LUMO orbital energies, can be expressed as: $I = -E_{HOMO}$, $A = -E_{LUMO}$, and the hardness (η) and the chemical potential (μ) are given the formula: $\eta = (I-A)/2$ and $\mu = -(I+A)/2$, where I and A are the first ionization potential and electron affinity of the chemical species. For the title compound, E_{HOMO} = -5.26043eV and E_{LUMO} = -2.056879 eV, Ionization potential (I) = 5.26043 eV, Electron affinity (A) = 2.05687 eV, Chemical hardness (η) = 1.60178 eV, Softness (s) = 0.624305 eV^{-1}, Chemical potential (μ) = -3.65865 eV, Electrophilicity index (ω) = 4.178388. It is seen that the chemical potential of the title compound is negative and it means that the compound is stable.

D. Molecular electrostatic potential (MEP)

Molecular electrostatic potential of a molecule has always verified to be a good guide in evaluating the molecules reactivity towards positively or negatively charged reactants, despite of the fact that the molecular charge distribution collected through the external test charge [45, 46]. To predict reactive sites of electrophilic and nucleophilic attacks for the investigated molecule, MEP at the B3LYP level optimized geometry was calculated. The different values of electrostatic potential at the MEP surface are characterized by different colors: red, blue and green represent the regions of most negative, most positive and zero electrostatic potential, respectively. The negative electrostatic potential resembles to an attraction of the proton by the cumulative electron density in the molecule (red shades), while the positive electrostatic potential represents to the repulsion of the proton by the atomic nuclei (blue shade). If the surface is largely white or lighter color shades, the molecule is mostly non-polar. The potential increases in the order of red < orange < yellow < green < blue. The negative regions (red, orange and yellow) of the MEP are related to electrophilic reactivity as shown in Fig.6. The maximum negative region is localized over the sulphur atoms and N-N- …. N atom of triazole ring and the maximum positive region is localized on NH group, indicating a possible site for nucleophilic attack. These sites give information about the region from which the compound can has intermolecular interactions. This predicted the most reactive site for both electrophilic and nucleophilic attack.

E. Natural bond orbital analysis

NBO analysis is based on a method for optimally transmuting a given wave functions into localized from, equivalent to the lone pairs and bonds of the Lewis structure picture [47]. In natural bond orbital analysis, the input atomic orbital basis set is transformed via natural atomic orbital and natural hybrid orbital into natural bond orbital. The NBO's obtained in this fashion correspond to the widely used Lewis picture, in which two center bonds and lone pairs are localized [48].

The natural bond orbital calculations were performed using NBO 3.1 program as implemented in the Gaussian09 package at the DFT/B3LYP level in order to understand various second order interactions between the filled orbital of one subsystem and vacant orbital of another subsystem. In the NBO analysis, the electronic wavefunctions are interpreted in terms of a set of occupied Lewis and set on non-Lewis localized orbital [49]. Delocalization effects can be recognized from the presence of off diagonal elements of the Fock matrix in the NBO basis. The output attained by the second order perturbation theory analysis normally the first to be observed by the experience NBO user in searching for substantial delocalization effects. The strength of these delocalization interactions E(2), are estimated by second order perturbation theory as estimated by the equation,

$$E(2) = \Delta E_{ij} = q_i \frac{F(ij)^2}{E_j - E_i}$$

q_i is the donor orbital occupancy, E_i and E_j are the diagonal elements and F_{ij} is the off diagonal NBO Fock matrix elements. The change in electron density (ED) in the (σ^*, π^*) antibonding orbitals and E(2) energies have been calculated by natural bond orbital (NBO) analysis using DFT method to give clear evidence of stabilization originating from various molecular interactions. The larger E(2) value in NBO analysis shows the intensive interaction between electron-donors and electron-acceptors, i.e. the more donation tendency from electron donors to electron acceptor and greater the extent of conjugation of the whole system. The second order perturbation theory analysis of Fock matrix in NBO basis shows strong intra-molecular hyper-conjugative interactions of π-electrons. NBO analysis has been performed on the title molecule at the B3LYP level in order to elucidate, the intra-molecular re-hybridization and delocalization of electron density within the molecule. In our study, the intramolecular hyperconjugative (interaction of the electrons in a sigma bond) interaction of $\sigma(C_1-C_2)$ distributed to $\sigma^*(C_1-C_9)$ resulting the stabilization energy of 3.08 kcal/mole are shown in Table 3. This enhanced further conjugation with the $\pi^*(C_1-C_2)$ antibonding orbital with a stabilization energy of 27.61 kcal/mole. From the title compound, σ (C_3 - C_4) → σ^*(C_1 - C_2), σ(C_{35} - C_{37}) → σ^*(C_{31} - C_{33}), σ(N_{12} - C_{14}) → σ^*(C_9 - C_{11}) and σ(C_9 - C_{11}) → σ^*(N_{12} - C_{14}) shows the stabilisation energies 14.16 kcal/mole, 19.39 kcal/mole, 26.26 kcal/mole and 35.22 kcal/mole respectively. Similarly, $\pi(N_{16})$ → $\pi^*(N_{12}-C_{14})$, and $\pi(C_{13})$ → $\pi^*(C_9-C_{11})$ show stabilization energies of 58.51 kcal/mole and 95.02 kcal/mole respectively.

F. Nonlinear optical activity (NLO)

Organic molecules can able to manipulate photonic signal efficiently are of importance in technologies such as optical communication and computing process [50, 51]. Nonlinear optical activity arises from the interactions of electromagnetic fields in various media to produce new fields altered in phase, amplitude, frequency or other propagation characteristic from the incident fields. In the field of technology measurement, there is an increasing interest in designing new organic materials with desired nonlinear optical properties. The first order hyperpolarizability (β) of the title molecule is calculated using B3LYP method. The dipole moment (μ), the statistic polarizability (α_0) and first static hyperpolarizability (β_{tot}) are related directly to the non-linear optical (NLO) activity of molecular structures. NLO activities of molecules have also reverse relationship with their biological activities.

The calculated values of the polarizabilities and the hyper polarizabilities from Gaussian 09 output were converted from atomic units into electrostatic units [52].

The total dipole moment (μ) = $(\mu_x^2 + \mu_x^2 + \mu_x^2)^{1/2}$

The calculation of static polarizability (α_{ave})

$\Delta\alpha = 1/3\ (\alpha_{xx} + \alpha_{yy} + \alpha_{zz})$

and first static hyper polarizability (β_{tot}) from Gaussian output, [53]

$$\beta_{tot} = [(\beta_{xxx} + \beta_{xyy} + \beta_{xzz})^2 + (\beta_{yyy} + \beta_{yzz} + \beta_{yxx})^2 + (\beta_{zzz} + \beta_{zxx} + \beta_{zyy})^2]^{1/2}$$

The calculated (β_{tot}) and $\Delta\alpha$ and ground state dipole moment were computed to be 12.67×10^{-30} esu and -150.63613 esu. The calculated values

for the title compound using B3LYP for the total hyperpolarizability (β_{tot}), dipole moment μ_i = (i= x,y,z), polarizability α_0 components are given in Table 4. The calculated dipole

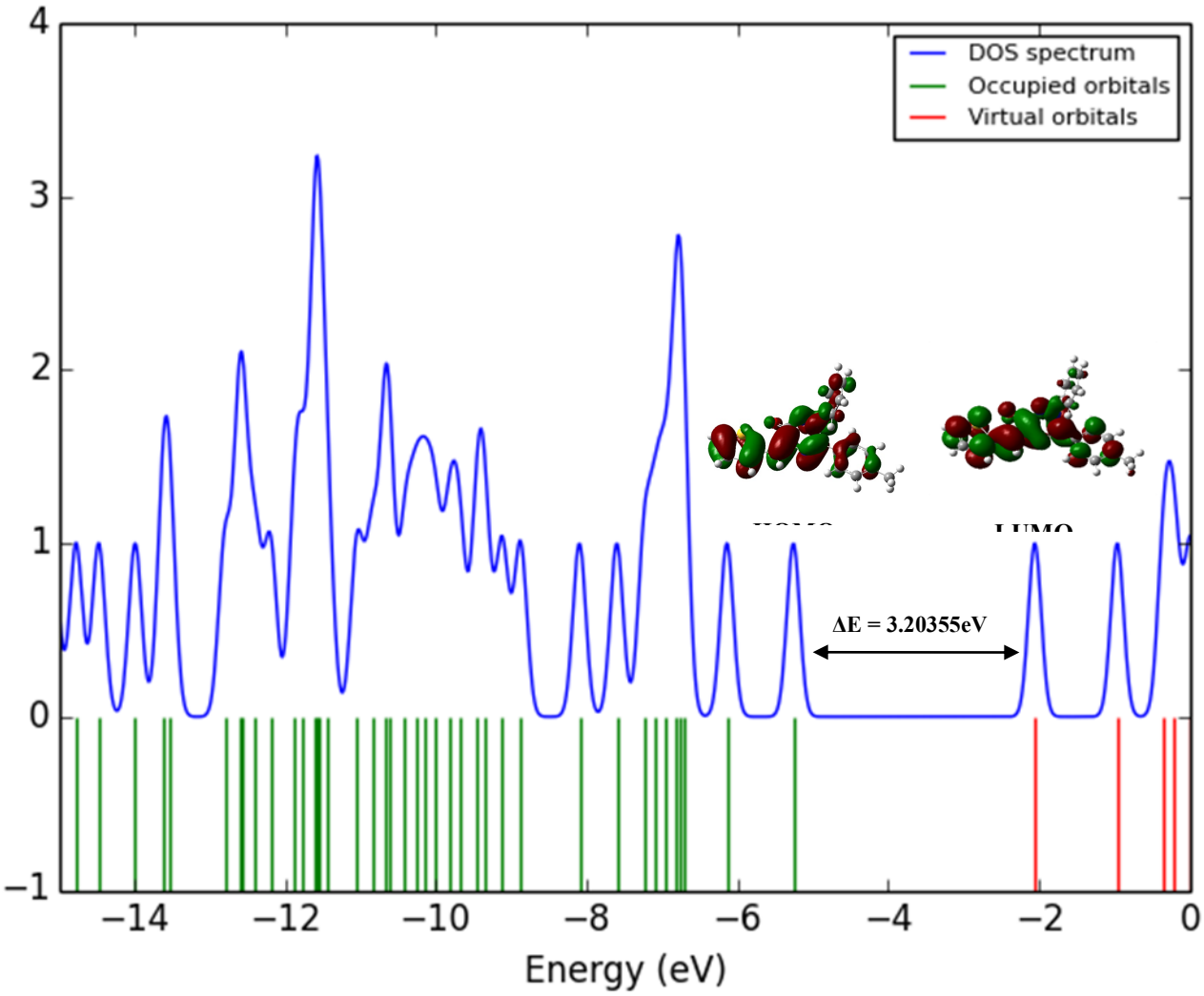

Fig. 4 DOS plots of Frontier Molecular Orbitals of 3-(4-Methylphenyl)-2-phenyl-5-(thiophen-2-ylmethylidene)-2, 5-dihydro-1, 2, 4-triazin-6(1*H*)-one

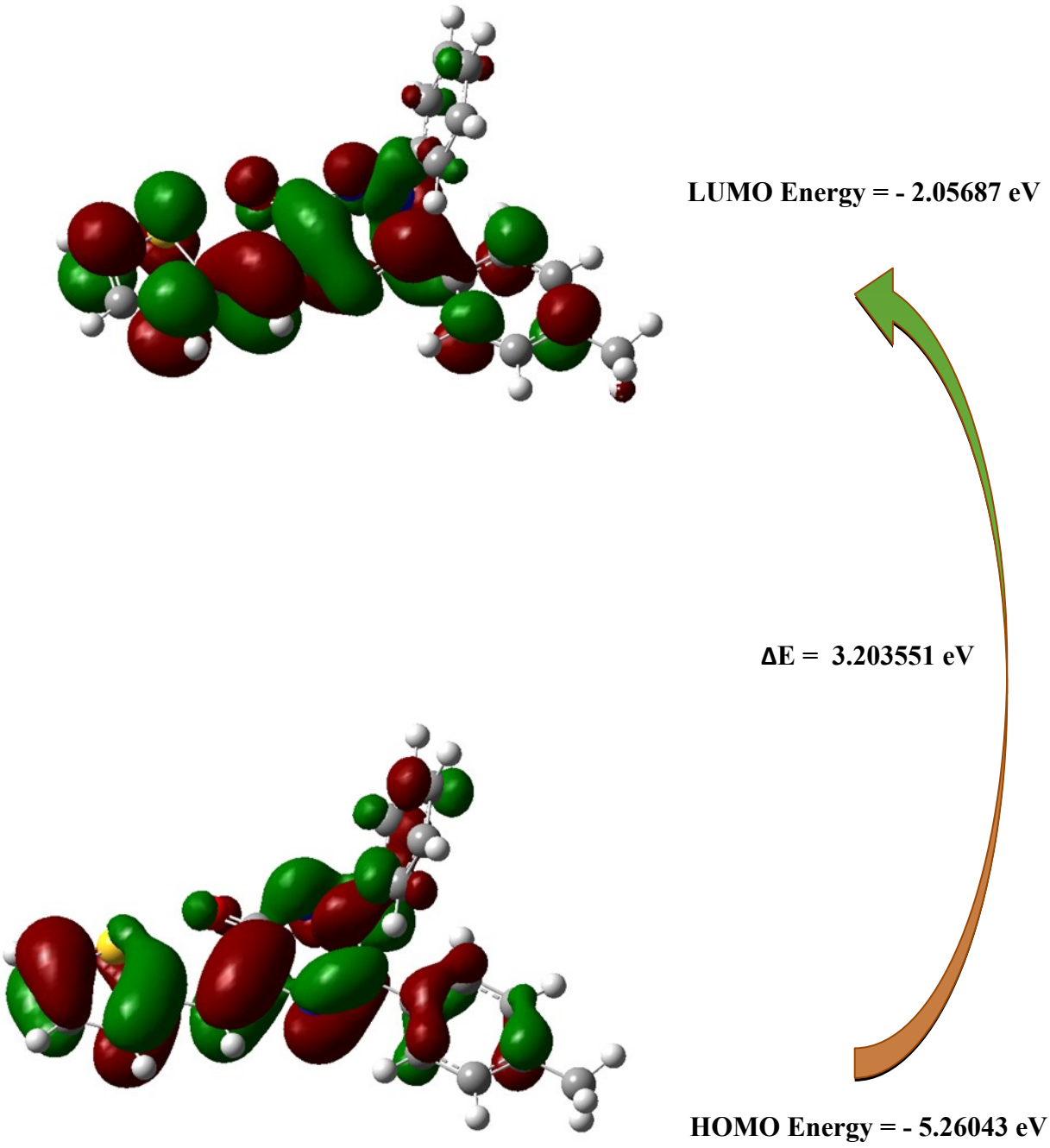

Fig. 5 HOMO-LUMO plot of 3-(4-Methylphenyl)-2- phenyl-5-(thiophen-2-ylmethylidene)-2, 5-dihydro-1, 2, 4-triazin-6(1*H*)-one

Table 3. Significant second-order interaction energy (E (2), kcal/mol) between donor and acceptor orbitals of 3-(4-Methylphenyl)-2-phenyl-5-(thiophen-2-ylmethylidene)-2,5-dihydro-1,2,4-triazin-6(1H)-one.

Donor (i)	Acceptor (j)	E(2)[a] kcal/mol	$(\varepsilon_i - \varepsilon_j)$[b] a.u	F_{ij}[c] a.u	Donor (i)	Acceptor (j)	E(2)[a] kcal/mol	$(\varepsilon_i - \varepsilon_j)$[b] a.u	F_{ij}[c] a.u	Donor (i)	Acceptor (j)	E(2)[a] kcal/mol	$(\varepsilon_i - \varepsilon_j)$[b] a.u	F_{ij}[c] a.u
σ(C1 - C2)	σ*(C1 - C9)	3.08	1.11	0.052	σ(C19 - C20)	σ*(C19 - C21)	4.39	1.28	0.067	σ(C30 - C32)	σ*(C31 - C33)	21.5	0.28	0.069
σ(C1 - C2)	σ*(C3 - C4)	18.23	0.27	0.064	σ(C19 - C21)	σ*(C19 - C20)	4.38	1.28	0.067	σ(C30 - C32)	σ*(C35 - C37)	18.71	0.28	0.065
σ(C1 - C2)	σ*(C9 - C11)	15.43	0.21	0.054	σ(C19 - C21)	σ*(N15 - N16)	3.81	0.62	0.047	σ(C31 - C33)	σ*(C14 - C30)	3.78	1.07	0.057
σ(C1 - S5)	σ*(C2 - H6)	3.63	1.19	0.059	σ(C19 - C21)	σ*(C20 - C22)	21.46	0.29	0.071	σ(C31 - C33)	σ*(30 - C31)	3.39	1.27	0.059
σ(C1 - S5)	σ*(C4 - H8)	3.42	1.19	0.057	σ(C19 - C21)	σ*(C24 - C26)	17.59	0.29	0.064	σ(C31 - C33)	σ*(C33 - C37)	3.27	1.28	0.058
σ(C1 - C9)	σ*(C1 - C2)	3.33	1.21	0.057	σ(C20 - C22)	σ*(N16 - C19)	4.95	1.02	0.064	σ(C31 - C33)	σ*(C37 - C40)	3.34	1.07	0.053
σ(C2 - C3)	σ*(C1 - C9)	4.93	1.04	0.064	σ(C20 - C22)	σ*(C19 - C20)	3.18	1.27	0.057	σ(C31 - C33)	σ*(C30 - C32)	20.46	0.28	0.068
σ(C2 - C3)	σ*(C4 - H8)	3.54	1.12	0.056	σ(C20 - C22)	σ*(C19 - C21)	20.65	0.27	0.067	σ(C31 - C33)	σ*(C35 - C37)	22.4	0.28	0.071
σ(C2 - H6)	σ*(C1 - S5)	4.73	0.76	0.054	σ(C20 - C22)	σ*(C24 - C26)	20.82	0.28	0.069	σ(C31 - H34)	σ*(C30 - C32)	4.13	1.09	0.06
σ(C3 - C4)	σ*(C1 - C2)	14.16	0.29	0.061	σ(C20 - H23)	σ*(C19 - C21)	4.17	1.08	0.06	σ(C32 - C35)	σ*(C14 - C30)	3.73	1.07	0.057
σ(C3 - H7)	σ*(C4 - S5)	3.88	0.77	0.049	σ(C20 - H23)	σ*(C22 - C26)	3.51	1.09	0.055	σ(C32 - H36)	σ*(C30 - C31)	4.14	1.09	0.06
σ(C4 - S5)	σ*(C1 - C9)	4.46	1.1	0.063	σ(C21 - C24)	σ*(N16 - C19)	4.92	1.02	0.064	σ(C33 - H38)	σ*(C35 - C37)	4.1	1.1	0.06
σ(C4 - S5)	σ*(C3 - H7)	4.04	1.18	0.062	σ(C21 - C24)	σ*(C19 - C21)	3.16	1.27	0.057	σ(C35 - C37)	σ*(C30 - C32)	22.51	0.28	0.071
σ(C9 - H10)	σ*(C1 - S5)	3.83	0.76	0.048	σ(C21 - H25)	σ*(C24 - C26)	3.5	1.09	0.055	σ(C35 - C37)	σ*(C31 - C33)	19.39	0.28	0.066
σ(C9 - C11)	σ*(N12 - C14)	3.92	1.06	0.058	σ(C22 - H27)	σ*(C19 - C20)	3.78	1.08	0.057	σ(C35 - H39)	σ*(C33 - C37)	4.11	1.1	0.06
σ(C9 - C11)	σ*(C13 - N15)	3.77	0.99	0.055	σ(C22 - H27)	σ*(C24 - C26)	3.57	1.09	0.056	σ(C40 - H42)	σ*(C35 - C37)	3.64	0.54	0.043
σ(C9 - C11)	σ*(C1 - C2)	18.25	0.2	0.053	σ(C24 - C26)	σ*(C19 - C21)	23.71	0.27	0.071	π(S5)	π*(C1 - C2)	27.61	0.26	0.077
σ(C9 - C11)	σ*(N12 - C14)	35.22	0.15	0.065	σ(C24 - C26)	σ*(C20 - C22)	19.85	0.28	0.067	π(S5)	π*(C3 - C4)	26.92	0.25	0.075
σ(C11 - N12)	σ*(C14 - C30)	3.41	1.2	0.057	σ(C24 - H28)	σ*(C19 - C21)	3.77	1.08	0.057	π(N12)	π*(C11 - C13)	8.44	0.87	0.078
σ(N12 - C14)	σ*(C9 - C11)	3.57	1.22	0.059	σ(C24 - H28)	σ*(C22 - C26)	3.58	1.09	0.056	π(N12)	π*(C14 - N16)	15.02	0.77	0.097
σ(N12 - C14)	σ*(C9 - C11)	26.26	0.27	0.08	σ(C26 - H29)	σ*(C20 - C22)	3.6	1.09	0.056	π(C13)	π*(C9 - C11)	95.02	0.08	0.094
σ(C13 - N15)	σ*(N16 - C19)	3.16	1.13	0.054	σ(C26 - H29)	σ*(C21 - C24)	3.61	1.09	0.056	π(N16)	π*(N12 - C14)	58.51	0.28	0.114
σ(C14 - C30)	σ*(C11 - N12)	3.17	1.13	0.054	σ(C30 - C31)	σ*(C30 - C32)	4.25	1.28	0.066	π(N16)	π*(C19 - C20)	4.81	0.84	0.062
σ(C14 - C30)	σ*(N15 - N16)	4.95	0.96	0.062	σ(C30 - C32)	σ*(C30 - C31)	4.25	1.28	0.066	π(N16)	π*(C19 - C21)	4.92	0.84	0.063
σ(N15 - H17)	σ*(C14 - N16)	3.79	1.09	0.058	σ(C30 - C32)	σ*(N12 - C14)	3.05	0.72	0.045	π(O18)	π*(C11 - C13)	6.83	0.74	0.065
σ(N16 - C19)	σ*(N12 - C14)	3.45	1.26	0.059	σ(C30 - C32)	σ*(C14 - N16)	4.06	0.69	0.051	π(O18)	π*(C13 - N15)	15.7	0.59	0.087

Donor (i)	Acceptor (j)	E(2)[a] kcal/mol	$(\varepsilon_i - \varepsilon_j)$[b] a.u	F_{ij}[c] a.u	Donor (i)	Acceptor (j)	E(2)[a] kcal/mol	$(\varepsilon_i - \varepsilon_j)$[b] a.u	F_{ij}[c] a.u	Donor (i)	Acceptor (j)	E(2)[a] kcal/mol	$(\varepsilon_i - \varepsilon_j)$[b] a.u	F_{ij}[c] a.u
σ(C1 - C2)	σ*(C1 - C9)	3.08	1.11	0.052	σ(C19 - C20)	σ*(C19 - C21)	4.39	1.28	0.067	σ(C30 - C32)	σ*(C31 - C33)	21.5	0.28	0.069
σ(C1 - C2)	σ*(C3 - C4)	18.23	0.27	0.064	σ(C19 - C21)	σ*(C19 - C20)	4.38	1.28	0.067	σ(C30 - C32)	σ*(C35 - C37)	18.71	0.28	0.065
σ(C1 - C2)	σ*(C9 - C11)	15.43	0.21	0.054	σ(C19 - C21)	σ*(N15 - N16)	3.81	0.62	0.047	σ(C31 - C33)	σ*(C14 - C30)	3.78	1.07	0.057
σ(C1 - S5)	σ*(C2 - H6)	3.63	1.19	0.059	σ(C19 - C21)	σ*(C20 - C22)	21.46	0.29	0.071	σ(C31 - C33)	σ*(30 - C31)	3.39	1.27	0.059
σ(C1 - S5)	σ*(C4 - H8)	3.42	1.19	0.057	σ(C19 - C21)	σ*(C24 - C26)	17.59	0.29	0.064	σ(C31 - C33)	σ*(C33 - C37)	3.27	1.28	0.058
σ(C1 - C9)	σ*(C1 - C2)	3.33	1.21	0.057	σ(C20 - C22)	σ*(N16 - C19)	4.95	1.02	0.064	σ(C31 - C33)	σ*(C37 - C40)	3.34	1.07	0.053
σ(C2 - C3)	σ*(C1 - C9)	4.93	1.04	0.064	σ(C20 - C22)	σ*(C19 - C20)	3.18	1.27	0.057	σ(C31 - C33)	σ*(C30 - C32)	20.46	0.28	0.068
σ(C2 - C3)	σ*(C4 - H8)	3.54	1.12	0.056	σ(C20 - C22)	σ*(C19 - C21)	20.65	0.27	0.067	σ(C31 - C33)	σ*(C35 - C37)	22.4	0.28	0.071
σ(C2 - H6)	σ*(C1 - S5)	4.73	0.76	0.054	σ(C20 - C22)	σ*(C24 - C26)	20.82	0.28	0.069	σ(C31 - H34)	σ*(C30 - C32)	4.13	1.09	0.06
σ(C3 - C4)	σ*(C1 - C2)	14.16	0.29	0.061	σ(C20 - H23)	σ*(C19 - C21)	4.17	1.08	0.06	σ(C32 - C35)	σ*(C14 - C30)	3.73	1.07	0.057
σ(C3 - H7)	σ*(C4 - S5)	3.88	0.77	0.049	σ(C20 - H23)	σ*(C22 - C26)	3.51	1.09	0.055	σ(C32 - H36)	σ*(C30 - C31)	4.14	1.09	0.06
σ(C4 - S5)	σ*(C1 - C9)	4.46	1.1	0.063	σ(C21 - C24)	σ*(N16 - C19)	4.92	1.02	0.064	σ(C33 - H38)	σ*(C35 - C37)	4.1	1.1	0.06
σ(C4 - S5)	σ*(C3 - H7)	4.04	1.18	0.062	σ(C21 - C24)	σ*(C19 - C21)	3.16	1.27	0.057	σ(C35 - C37)	σ*(C30 - C32)	22.51	0.28	0.071
σ(C9 - H10)	σ*(C1 - S5)	3.83	0.76	0.048	σ(C21 - H25)	σ*(C24 - C26)	3.5	1.09	0.055	σ(C35 - C37)	σ*(C31 - C33)	19.39	0.28	0.066
σ(C9 - C11)	σ*(N12 - C14)	3.92	1.06	0.058	σ(C22 - H27)	σ*(C19 - C20)	3.78	1.08	0.057	σ(C35 - H39)	σ*(C33 - C37)	4.11	1.1	0.06
σ(C9 - C11)	σ*(C13 - N15)	3.77	0.99	0.055	σ(C22 - H27)	σ*(C24 - C26)	3.57	1.09	0.056	σ(C40 - H42)	σ*(C35 - C37)	3.64	0.54	0.043
σ(C9 - C11)	σ*(C1 - C2)	18.25	0.2	0.053	σ(C24 - C26)	σ*(C19 - C21)	23.71	0.27	0.071	π(S5)	π*(C1 - C2)	27.61	0.26	0.077
σ(C9 - C11)	σ*(N12 - C14)	35.22	0.15	0.065	σ(C24 - C26)	σ*(C20 - C22)	19.85	0.28	0.067	π(S5)	π*(C3 - C4)	26.92	0.25	0.075
σ(C11 - N12)	σ*(C14 - C30)	3.41	1.2	0.057	σ(C24 - H28)	σ*(C19 - C21)	3.77	1.08	0.057	π(N12)	π*(C11 - C13)	8.44	0.87	0.078
σ(N12 - C14)	σ*(C9 - C11)	3.57	1.22	0.059	σ(C24 - H28)	σ*(C22 - C26)	3.58	1.09	0.056	π(N12)	π*(C14 - N16)	15.02	0.77	0.097
σ(N12 - C14)	σ*(C9 - C11)	26.26	0.27	0.08	σ(C26 - H29)	σ*(C20 - C22)	3.6	1.09	0.056	π(C13)	π*(C9 - C11)	95.02	0.08	0.094
σ(C13 - N15)	σ*(N16 - C19)	3.16	1.13	0.054	σ(C26 - H29)	σ*(C21 - C24)	3.61	1.09	0.056	π(N16)	π*(N12 - C14)	58.51	0.28	0.114
σ(C14 - C30)	σ*(C11 - N12)	3.17	1.13	0.054	σ(C30 - C31)	σ*(C30 - C32)	4.25	1.28	0.066	π(N16)	π*(C19 - C20)	4.81	0.84	0.062
σ(C14 - C30)	σ*(N15 - N16)	4.95	0.96	0.062	σ(C30 - C32)	σ*(C30 - C31)	4.25	1.28	0.066	π(N16)	π*(C19 - C21)	4.92	0.84	0.063
σ(N15 - H17)	σ*(C14 - N16)	3.79	1.09	0.058	σ(C30 - C32)	σ*(N12 - C14)	3.05	0.72	0.045	π(O18)	π*(C11 - C13)	6.83	0.74	0.065
σ(N16 - C19)	σ*(N12 - C14)	3.45	1.26	0.059	σ(C30 - C32)	σ*(C14 - N16)	4.06	0.69	0.051	π(O18)	π*(C13 - N15)	15.7	0.59	0.087

Table 4. The *Ab initio* B3LYP/ 6-31G and B3LYP/6-311G calculated electric dipole moments (Debye), Dipole moments compound, polarizability (in a.u), β components and β_{tot} (10^{-29} esu) value of 3-(4-Methylphenyl)-2-phenyl-5-(thiophen-2-ylmethylidene)-2,5-dihydro-1,2,4-triazin-6(1*H*)-one

Parameters	B3LYP/ 6-31G	B3LYP/ 6-311G	Parameters	B3LYP/ 6-31G	B3LYP/ 6-311G
μ_x	8.5353	8.6580	β_{xxx}	44.4670	45.3894
μ_y	0.6305	0.7057	β_{yyy}	11.8592	13.1429
μ_z	2.0458	2.1498	β_{zzz}	10.8738	11.6195
μ	8.7996	8.9488	β_{xyy}	92.2589	94.6923
α_{xx}	-139.8562	-142.4200	β_{xxy}	53.6665	54.9837
α_{yy}	-159.8385	-163.9948	β_{xxz}	18.2646	18.4351
α_{zz}	-143.3464	-145.4936	β_{xzz}	6.8022	7.5002
α_{xy}	-18.7111	-18.9087	β_{yzz}	0.0662	0.1309
α_{xz}	-4.0822	-4.4645	β_{YYZ}	17.9209	18.4473
α_{yz}	-2.9049	-2.8373	β_{XYZ}	7.7413	8.0573
$\Delta\alpha$(esu)	-147.68037	-150.63613	βtot(esu)	12.3×10^{-30}	12.67×10^{-30}

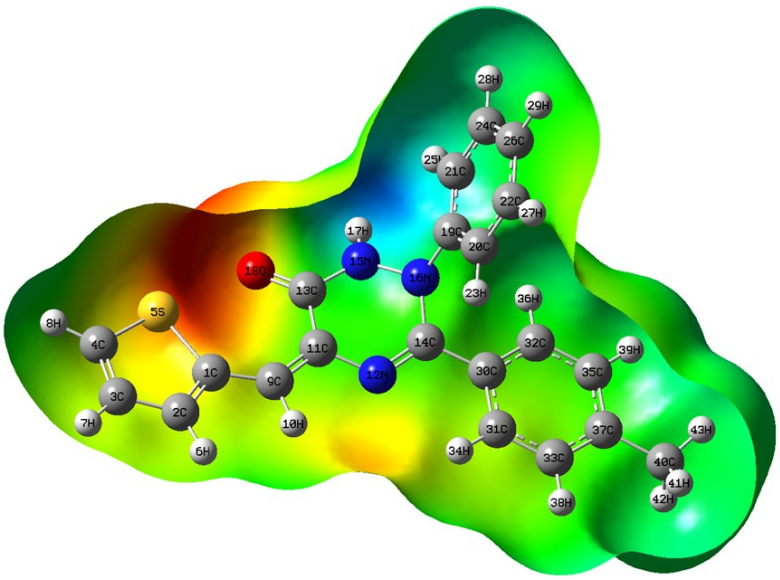

Fig. 6 Molecular Electrostatic Potential map of 3-(4-Methylphenyl)-2-phenyl-5-(thiophen-2-ylmethylidene)-2, 5-dihydro-1, 2, 4-triazin-6(1*H*)-one

147.68037 esu. The hyperpolarizability β controlled by the longitudinal components of β_{xxx}, β_{yyy}, β_{xyy}, β_{xxy}, and β_{yyz}. The large values of components of polarizability and hyperpolarizability indicate significant delocalization of charges in these directions.

G. Nuclear Magnetic Resonance (NMR)

NMR is a most valuable technique for structural characterization in thiophene

derivatives, subsequently spectral interpretation is predominantly much easier in the thiophene series compared to benzene derivatives. ^{1}H and ^{13}C NMR spectroscopy can provide the required structural data for the compound [54, 55]. The experimental ^{1}H and ^{13}C spectra were shown in Fig. 7. Chemical shifts in proton NMR are well-documented and the coupling constants (J) in substituted thiophene occur in well-defined ranges; 1.0, 2.8, 3.5 and 4.8 Hz [56]. Hence, assignment of the aromatic protons of the thiophene ring was readily carried out based on coupling constants in the present study.

Taking into the account that the range of ^{13}C NMR chemical shifts for a typical aromatic organic molecule usually is >100 ppm [57, 58]. It determines physical and chemical properties of atoms or molecules. If the number of neutrons and the number of protons are both even, the nucleus has no spin. If the number of neutrons plus the number of protons is odd, then the nucleus has a half-integer spin (i.e. 1/2, 3/2, 5/2). If the number of neutrons and the number of protons are both odd, then the nucleus has an integer spin (i.e. 1, 2, and 3). The hydrogen atoms are mostly localized on periphery of the molecules and their chemical shifts would be more susceptible to intermolecular interactions as compared to that for other heavier atoms. Unsaturated carbons give signals in overlapped areas of the spectrum with chemical shift values from 100 to 200 ppm. The ^{13}C NMR spectra exhibit signals somewhat downfield of 170 ppm depending on the structure. Such signals are typically weak due to the absence of nuclear Overhauser effects. The external magnetic field experienced by the carbon nuclei is affected by the electronegativity of the atoms attached to them. The carbonyl carbon atom C_{13} in the title molecule show very downfield effect and the corresponding observed chemical shift is 168.87 ppm. The more electronegative character of the oxygen atoms renders a positive charge to the carbon and thus C1 chemical shift is observed in the more downfield shift at 159.33 ppm. The chemical shift values of other carbon atoms of the title compound are observed at 147.04, 137.86, 134.84, 128.32 and 120.51 ppm. The ^{1}H chemical shifts of the title molecule are obtained by complete analysis of their NMR spectra and interpreted critically in an attempt to quantify the possible different effects acting on the shielding constant and in turn to the chemical shift of protons. ^{1}H NMR spectra of the title compound indicates, the hydrogen atoms are attached with the aromatic carbons in which the peak values at 9.031, 8.112, 8.012, 7.346, 7.194, 6.811 and 6.687 ppm. The experimental ^{1}H and ^{13}C NMR chemical shifts are represented in the Fig.7.

H. Fukui function

The Fukui function is a local reactivity descriptor that predicts the desired region where a chemical species will change its density when the number of electrons is modified and it indicates the propensity of the electronic density to deform at a given position upon accepting or donating electrons [59-61].

Also, it is possible to define the corresponding condensed or atomic Fukui-functions on the j^{th} atom site as

$$f_j^+ = q_j(N+1) - q_j(N)$$

$$f_j^- = q_j(N) - q_j(N-1)$$

$$f_j^0 = \frac{1}{2}[q_j(N+1) - q_j(N-1)]$$

For an electrophilic f_j^- (r), nucleophilic or free radical attack f_j^+ (r), on the reference molecule, respectively. In these equation, q_j is the atomic charge (evaluated from Mulliken population analysis, electrostatic derived charge, etc.) at the j^{th} atomic site is the neutral (N), anionic (N+1) or cationic (N-1) chemical species. Chattaraj et al. [62] proposed the idea of generalized philicity and it contains almost all information about the known different global and local reactivity and selectivity descriptor, in addition to the information regarding electrophilic/nucleophilic power of a given atomic site in a molecule. Morell et al. [63] have proposed a dual descriptor ($\Delta f(r)$), which is defined as the difference between the nucleophilic and electrophilic Fukui function and in given by,

$$\Delta f(r) = [f^+(r) - f^-(r)]$$

If $\Delta f(r) > 0$, then the site is favoured for a nucleophilic attack,

$\Delta f(r) < 0$, then the site may be favoured for an electrophilic attack.

$\Delta f(r)>0$, then the site is favoured for a nucleophilic attack, whereas if $\Delta f(r)<0$, then the site may be favoured for an electrophilic attack. According to dual descriptor $\Delta f(r)$ provide a clear difference between nucleophilic and electrophilic attack at a particular site with their sign. That is, they provide positive value for sited prone for nucleophilic attack and a negative value prone for electrophilic attack and these values are reported in the Table 5. From the condition for dual descriptor, nucleophilic sites for in our title molecule are C2, C4, H8, C9, C11, N12, N15, N16, O18, C22, C24, C40 (positive value i.e. $\Delta f(r) >0$). Similarly, the electrophilic sites are C1, C3, S5, H6, H7, H10, C13, C14, H17, C19, C20, C21, H23, H25, H27, H28, H29, C30, C31, C32, C33, H34, H36, C37, H38, H39, H41, H42, H43 (Negative i.e. $\Delta f (r)<0$). The behaviour of molecule as electrophilic and nucleophilic attack during reaction depends on the local behaviour of molecules.

I. Mulliken Charges

The calculation of atomic charges plays a significant role in the application of quantum mechanical calculations to molecular systems. Mulliken charges are calculated by determining the electron population of each atom as defined in the basis functions. The charge distributions calculated by the Mulliken [64] and NBO methods for the equilibrium geometry of 3-(4-Methylphenyl)-2-phenyl-5-(thiophen-2-ylmethylidene)-2,5-dihydro-1,2,4-triazin-6(1*H*)-one are given in the Table 6 and as shown in Fig. 8. The charge distribution on the molecule has an important impact on the vibrational spectra. The Mulliken atomic charges were calculated by the DFT/B3LYP method with 6-31G and 6-311G basis sets. This calculation represents the charges of every atom in the title molecule. The magnitudes of the carbon atoms connected to hydrogen atoms were found to be generally negative value and the carbon atoms connected to oxygen and nitrogen atoms were calculated to be negative value as expected. In the title compound, the Mulliken atomic charge of the carbon atoms like C_{13}, C_{14} and C_{19} become more positive, shows the direction of delocalization and shows that the natural atomic charges are more sensitive to the changes in the molecular structure.

J. Magnetic susceptibility

Atoms, molecules, free radicals or ions which contain one or more unpaired electron will possess permanent magnetic dipole moment that arises from the residual spin and angular moment of the unpaired electrons. All substances having permanent magnetic moment display paramagnetic behaviour in nature. When a paramagnetic substance is placed in a magnetic field, they will align themselves in the direction of the field and thus produces positive magnetic susceptibility, which depends on the temperature; since thermal agitation will oppose the alignment of the magnetic dipoles. The susceptibility is very small: 10^{-4} to 10^{-5}. The effectiveness of diminishes increases with increase in temperature. A paramagnetic compound will have some electrons with unpaired spins. Paramagnetism derives from the spin and orbital angular moment of electrons. This type of magnetism occurs only in compounds containing unpaired electrons, as the spin and orbital angular momenta is cancelled out when the electrons exist in pairs. The magnetic susceptibility (χ_m) of the molecules for various temperatures are predicted with knowledge of unpaired electron [65] and presented in Table 7. The graphical representation of ($1/\chi_m$) with T (temperature) is shown in Fig. 9. A plot of χ versus 1/ temperature is known as a Curie plot. Ideally, it should be linear if the Curie-Weiss law is obeyed. For the title compound the plot of χ versus 1/T is linear hence Curie-Weiss law is obeyed.

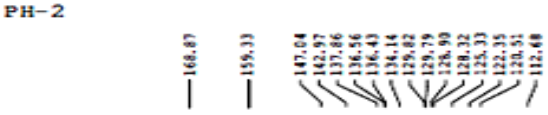

Table 5. Values of Fukui function considering Mulliken charges of 3-(4-Methylphenyl)-2-phenyl-5-(thiophen-2-ylmethylidene)-2,5-dihydro-1,2,4-triazin-6(1*H*)-one

Mulliken Atomic Charges (a.u)				Fukui's Function (a.u)				Atomic Softness			Electrophilicity Indices		
Atom	Neutral (N)	Cation (N-1)	Anion (N+1)	f_k^+	f_k^-	f_k^0	$\Delta f(r)$	s_k^+	s_k^-	s_k^0	ω_k^+	ω_k^-	ω_k^0
C1	-0.380	-0.459	-0.624	-0.2437	0.07872	-0.0825	-0.322	-0.094	0.030	-0.032	-0.797	0.257	-0.270
C2	-0.052	0.156	0.026	0.07791	-0.2079	-0.065	0.286	0.030	-0.080	-0.025	0.255	-0.680	-0.213
C3	-0.068	-0.015	-0.136	-0.0677	-0.0533	-0.0605	-0.014	-0.026	-0.021	-0.023	-0.221	-0.174	-0.198
C4	-0.503	-0.103	-0.173	0.32971	-0.3997	-0.035	0.729	0.127	-0.154	-0.013	1.078	-1.307	-0.114
S5	0.533	0.214	0.028	-0.5054	0.31944	-0.093	-0.825	-0.195	0.123	-0.036	-1.653	1.045	-0.304
H6	0.137	0.212	0.027	-0.1097	-0.0753	-0.0925	-0.034	-0.042	-0.029	-0.036	-0.359	-0.246	-0.302
H7	0.136	-0.499	-0.666	-0.802	0.63501	-0.0835	-1.437	-0.309	0.245	-0.032	-2.623	2.076	-0.273
H8	0.167	0.352	0.246	0.07859	-0.1846	-0.053	0.263	0.030	-0.071	-0.020	0.257	-0.604	-0.173
C9	-0.005	0.362	0.235	0.24042	-0.3674	-0.0635	0.608	0.093	-0.141	-0.024	0.786	-1.201	-0.208
H10	0.145	0.159	-0.196	-0.341	-0.014	-0.1775	-0.327	-0.131	-0.005	-0.068	-1.115	-0.046	-0.580
C11	0.002	0.831	0.737	0.73493	-0.8289	-0.047	1.564	0.283	-0.319	-0.018	2.403	-2.711	-0.154
N12	-0.343	-0.019	-0.037	0.30603	-0.324	-0.009	0.630	0.118	-0.125	-0.003	1.001	-1.060	-0.029
C13	0.531	0.555	0.492	-0.0395	-0.0235	-0.0315	-0.016	-0.015	-0.009	-0.012	-0.129	-0.077	-0.103
C14	0.313	-0.236	-0.301	-0.6139	0.54894	-0.0325	-1.163	-0.236	0.211	-0.013	-2.008	1.795	-0.106
N15	-0.498	-0.257	-0.315	0.18346	-0.2415	-0.029	0.425	0.071	-0.093	-0.011	0.600	-0.790	-0.095
N16	-0.484	-0.254	-0.314	0.16989	-0.2299	-0.03	0.400	0.065	-0.089	-0.012	0.556	-0.752	-0.098
H17	0.363	-0.251	-0.313	-0.6757	0.6137	-0.031	-1.289	-0.260	0.236	-0.012	-2.210	2.007	-0.101
O18	-0.532	-0.248	-0.312	0.21985	-0.2838	-0.032	0.504	0.085	-0.109	-0.012	0.719	-0.928	-0.105
C19	0.208	-0.245	-0.311	-0.5192	0.45317	-0.033	-0.972	-0.200	0.175	-0.013	-1.698	1.482	-0.108
C20	-0.071	-	-	-0.0572	0.00537	-0.0259	-0.063	-0.022	0.002	-0.010	-0.187	0.018	-0.085
C21	-0.071	-	-0.131	-0.0597	0.0141	-0.0228	-0.074	-0.023	0.005	-0.009	-0.195	0.046	-0.075
C22	-0.148	-	-	0.01437	-0.0538	-0.0197	0.068	0.006	-0.021	-0.008	0.047	-0.176	-0.064
H23	0.158	-	-	-0.2941	0.26093	-0.0166	-0.555	-0.113	0.100	-0.006	-0.962	0.853	-0.054
C24	-0.148	-	-	0.00888	-0.0359	-0.0135	0.045	0.003	-0.014	-0.005	0.029	-0.117	-0.044
H25	0.159	-	-	-0.3013	0.28045	-0.0104	-0.582	-0.116	0.108	-0.004	-0.985	0.917	-0.034
C26	-0.102	-	-0.145	-0.0434	0.02878	-0.0073	-0.072	-0.017	0.011	-0.003	-0.142	0.094	-0.024
H27	0.149	-	-	-0.2964	0.28803	-0.0042	-0.584	-0.114	0.111	-0.002	-0.969	0.942	-0.014
H28	0.149	-	-	-0.2992	0.29697	-0.0011	-0.596	-0.115	0.114	0.000	-0.978	0.971	-0.004
H29	0.146	-	-	-0.2989	0.30287	0.00199	-0.602	-0.115	0.117	0.001	-0.977	0.990	0.007
C30	0.030	-	-	-0.186	0.19621	0.00509	-0.382	-0.072	0.076	0.002	-0.608	0.642	0.017
C31	-0.114	-	-	-0.0445	0.06087	0.00819	-0.105	-0.017	0.023	0.003	-0.146	0.199	0.027
C32	-0.113	-	-	-0.0484	0.07099	0.01129	-0.119	-0.019	0.027	0.004	-0.158	0.232	0.037
C33	-0.157	-	-	-0.0074	0.03616	0.01439	-0.044	-0.003	0.014	0.006	-0.024	0.118	0.047
H34	0.138	-	-	-0.3048	0.33977	0.01748	-0.645	-0.117	0.131	0.007	-0.997	1.111	0.057
C35	-0.158	-	-	-0.0125	0.05372	0.02058	-0.066	-0.005	0.021	0.008	-0.041	0.176	0.067
H36	0.139	-	-	-0.3115	0.35887	0.02368	-0.670	-0.120	0.138	0.009	-1.019	1.174	0.077
C37	0.099	-	-	-0.2743	0.32787	0.02678	-0.602	-0.106	0.126	0.010	-0.897	1.072	0.088
H38	0.129	-	-	-0.3074	0.36718	0.02988	-0.675	-0.118	0.141	0.012	-1.005	1.201	0.098
H39	0.129	-	-	-0.3102	0.37616	0.03298	-0.686	-0.119	0.145	0.013	-1.014	1.230	0.108
C40	-0.468	-	-0.184	0.28416	-0.212	0.03608	0.496	0.109	-0.082	0.014	0.929	-0.693	0.118
H41	0.148	-	-	-0.3343	0.41266	0.03918	-0.747	-0.129	0.159	0.015	-1.093	1.349	0.128
H42	0.165	-	-	-0.3545	0.43903	0.04228	-0.794	-0.137	0.169	0.016	-1.159	1.436	0.138
H43	0.146	-	-	-0.3385	0.42925	0.04538	-0.768	-0.130	0.165	0.017	-1.107	1.404	0.148

Table 6. Mulliken population analysis of 3-(4-Methylphenyl)-2-phenyl-5-(thiophen-2-ylmethylidene)-2,5-dihydro-1,2,4-triazin-6(1*H*)-one performed at B3LYP/6-31G and B3LYP/6-311G

Atoms	Atomic Charges		Atoms	Atomic Charges	
	B3LYP/ 6-31G	B3LYP/ 6-311G		B3LYP/ 6-31G	B3LYP/ 6-311G
C1	-0.380281	-0.407846	H23	0.157535	0.175407
C2	-0.051905	-0.012178	C24	-0.148277	-0.173131
C3	-0.068325	-0.108639	H25	0.159085	0.1774
C4	-	-	C26	-	-

	0.502705	0.472353		0.101579	0.111562
S5	0.533441	0.417723	H27	0.148685	0.166413
H6	0.13671	0.16722	H28	0.148647	0.166279
H7	0.136012	0.164976	H29	0.145556	0.165246
H8	0.167409	0.201945	C30	0.029912	-0.075191
C9	-0.005421	0.048084	C31	-0.114412	-0.096542
H10	0.145018	0.174816	C32	-0.113279	-0.093062
C11	0.002073	-0.185267	C33	-0.1571	-0.131263
N12	-0.343029	-0.2666	H34	0.137531	0.155188
C13	0.53146	0.575157	C35	-0.157513	-0.134552
C14	0.312939	0.308387	H36	0.13866	0.157471
N15	-0.498457	-0.507926	C37	0.098672	0.021602
N16	-0.483889	-0.533249	H38	0.128991	0.154317
H17	0.362696	0.363982	H39	0.128992	0.154576
O18	-0.531849	-0.503156	C40	-0.468155	-0.600247
C19	0.208174	0.176957	H41	0.147518	0.189101
C20	-0.071065	-0.045797	H42	0.164899	0.208598
C21	-0.071322	-0.047062	H43	0.146136	0.187862
C22	-0.148189	-0.173086			

Table 7. Magnetic susceptibility of 3-(4-Methylphenyl)-2-phenyl-5-(thiophen-2-ylmethylidene)-2,5-dihydro-1,2,4-triazin-6(1*H*)-one at various temperatures.

S. No	Temperature (K)	Susceptibility (χ_m) mole per m^3	1/ Susceptibility $1/\chi$
1	50	4.24575E-06	235529.6473
2	100	2.12288E-06	471059.2946
3	150	1.41525E-06	706588.9419
4	200	1.06144E-06	942118.5892
5	250	8.4915E-07	1177648.236
6	298.15	7.12016E-07	1404463.287
7	350	6.06536E-07	1648707.531
8	400	5.30719E-07	1884237.178
9	450	4.7175E-07	2119766.826
10	500	4.24575E-07	2355296.473
11	550	3.85977E-07	2590826.12
12	600	3.53813E-07	2826355.768

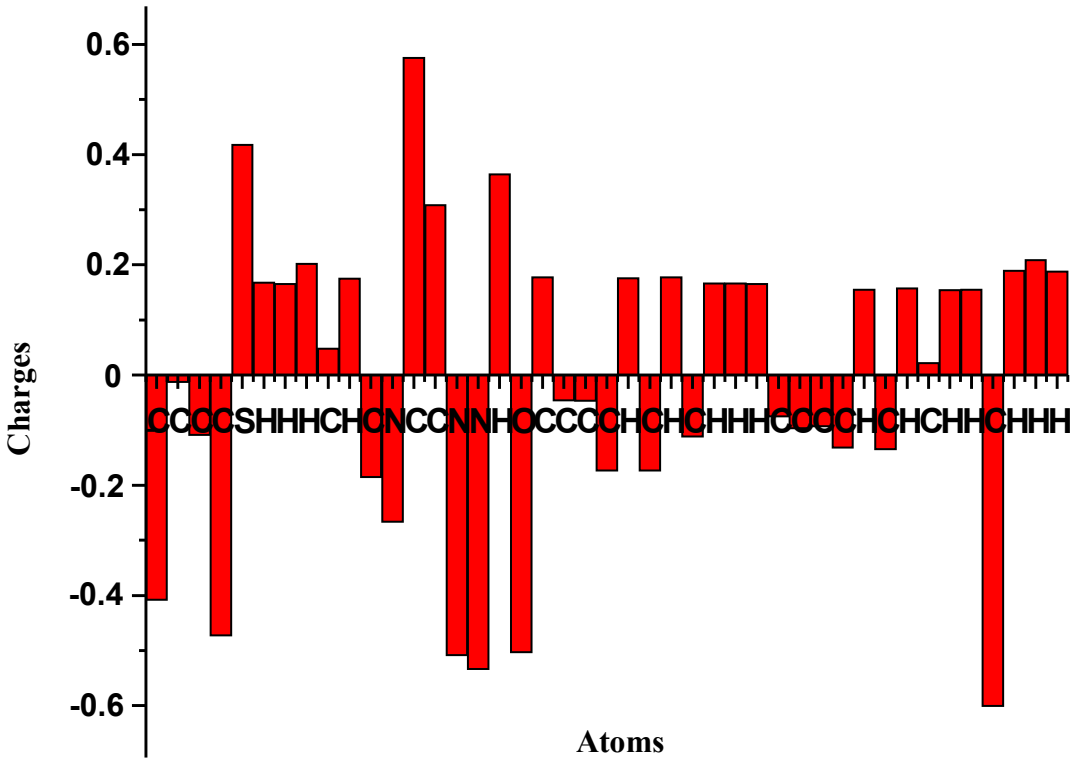

Fig. 8 Mulliken atomic charges of 3-(4-Methylphenyl)-2-phenyl-5-(thiophen-2-ylmethylidene)-2, 5-dihydro-1, 2, 4-triazin-6(1*H*)-one

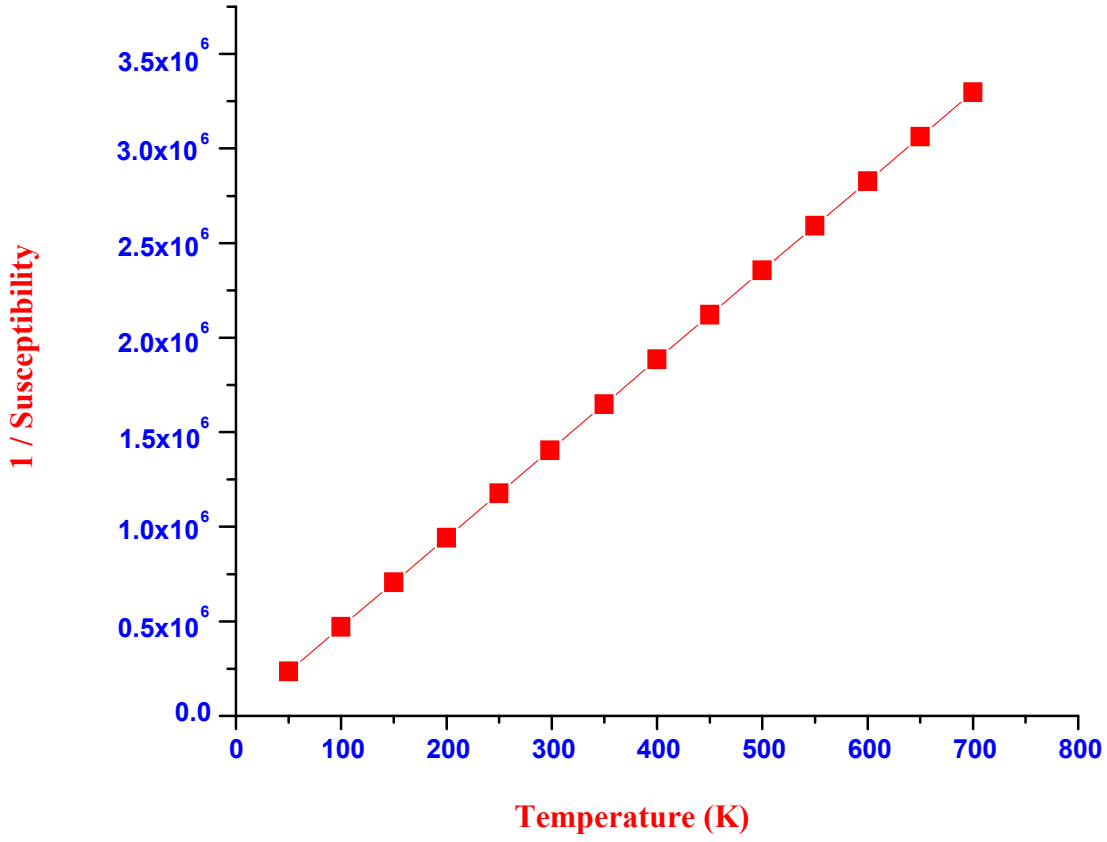

Fig. 9 Magnetic Susceptibility plot of 3-(4-Methylphenyl)-2- phenyl-5-(thiophen-2-ylmethylidene)-2, 5-dihydro-1, 2, 4-triazin-6(1*H*)-one

The following regression equation (linear equation) is measured to be the best fit to predict the value of Curie constant.

$$Y=4447x+8E\text{-}05 \quad (R2\text{-}I)$$

Curie constant = 0.00027, Weiss constant= 5.12379×10^{-07} (BM). The Weiss constant is almost zero. Hence the plot passes through the origin which proves the paramagnetic nature.

Conclusion

The vibrational properties of 3-(4-Methylphenyl)-2-phenyl-5-(thiophen-2-ylmethylidene)-2,5-dihydro-1,2,4-triazin-6(1*H*)-one have been examined using experimental techniques FT-IR and FT-Raman) and density functional theory calculation conducted by B3LYP/6-31G and B3LYP/6-311G basis sets method theoretically. The theoretically vibrational wavenumbers were compared with the experimental values, which yield good agreement with calculated values. The very good coherence has been observed between scaled wavenumbers and experimental wavenumbers. The theoretical support has been addressed by DFT calculations, and the peculiarities and limitations of the theoretical approach to the analysis have been considered. The complete assignments of fundamental modes were performed on the basis of potential energy distribution. The NBO analysis shows strong intermolecular hyper conjugative interaction of π electron in the molecule leading to stabilization of the molecule. HOMO-LUMO studies reveal the intra molecular charge transfer through conjugated system. The molecular stability increased by the interaction of the electrons in a sigma bond with antibonding sigma orbital and charge delocalization has evaluated. ^{1}H and ^{13}C NMR chemical shifts are experimentally analyzed. Above said sites give details about the region where the compound can have intermolecular interactions. We anticipate this work will be very useful for the design and synthesis new materials.

References

1. GK. Gribble, M.G. Saulnier, M.P. Sibi, J.A. Obaza-Nutaitis, synthesis and Diels-Alder reactions of 1, 3-dimethyl-4-(phenylsulfonyl)-4H-furo [3, 4-b] indole. A new annulation strategy for the construction of ellipticine and isoellipticine, J. Org.chem. 49 (1984) 4518 – 4523.
2. Press, J.B. Pharmacologically active compounds and other thiophene derivatives. In: Gronowitz S (ed), Chemistry of Hetero Cyclic Compounds: Thiophene and its derivatives, Pt, 1. Vol 44; John Wiley, New York, (1985) pp, 353 - 456.
3. J B. Press, Chemistry of heterocyclic compounds, in: S. Gronowitz (Ed.), Thiophene and its Derivatives, Part 4, Vol. 44, Wiley, New York, 1991, pp, 397-502.
4. IF. Perepichka, D.F. Perepichka (Eds). Handbook of thiophene-based materials, Wiley Chichester, U.K., 2009.
5. A Mishra, C.-Q. Ma, P. Bauerle, Fucntional oligothiophenes: molecular design for multidimensional nanoarchitectures and their applications, Chem. Rev. 109 (2009) 1141- 1276
6. Patel, R.V.; Kumari, P.; Rajani, D.P.; Pannecouque, C.; de Clercq, E.; Chikhalia, K.H. Antimicrobial, anti-TB, anticancer and anti-HIV evaluation of nefw s-triazine-based heterocycles. Future Med. Chem. 2012, 4, 1053-1065.
7. Khoshneviszadeh, M.; Mohammad, H.; Foroumadi, G.A.; Miri, R.; Firuzi, O.; Madadkar- Sobahani, A.; Edraki, N.; Parsa, M.; Shafiee, A. Design, synthesis and biological evaluation of novel anti-cytokine 1,2,4-tirazine derivatives. Bioorg. Med. Chem. 2013, 21, 6708-6717.
8. Gussian 09, Revision D.01, M.J. Frisch, G.W. Trucks, H.B. Schlegel, G.E. Scuseria, M.A. Robb, J.R. Cheeseman, G. Scalmani, V. Barone, B. Mennucci, G.A. Petersson, H. Nakatsuji, M. Caricato, X. Li, H.P. Hratchian, A.F. Izmaylov, J. Bloino, G. Zheng, J.L. Sonnenberg, M. Hada, M.

Ehara, K. Toyota, R. Fukuda, J. Hasegawa, M. Ishida, T. Nakajima, Y. Honda, O. Kitao, H. Nakai, T. Vreven, J.A. Montgomery, Jr., J.E. Peralta, F. Ogliaro, M. Bearpark, J.J. Heyd, E. Brothers, K.N. Kudin, V.N. Staroverov, T. Keith, R. Kobayashi, J. Normand, K. Raghavachari, A. Rendell, J.C. Burant, S.S. Iyengar, J. Tomasi, M. Cossi, N. Rega, J.M. Millam, M. Klene, J.E. Knox, J.B. Cross, V. Bakken, C.Adamo, J. Jaramillo, R. Gomperts, R.E. Stratmann, O. Yazyev, A.J. Austin, R. Cammi, C. Pomelli, J.W. Ochterski, R.L. Martin, K. Morokuma, V.G. Zakrzewski, G.A. Voth, P. Salvador, J.J. Dannenberg, S. Dapprich, A.D. Daniels, O. Farkas, J.B. Foresman, J.V. Ortiz, J. Cioslowski, D.J. Fox, Gaussian, Inc., Wal ngford CT, 2013.

9. A Irfan, R. Jin, A.G. Al-Sehemi, A.M. Asiri, Spectrochim. Acta 110 (2013) 60.
10. A. Irfan, A.G. Al-Sehemi, M.S. Al-Assiri, J. Fluor. Chem. 157 (2014) 52.
11. J.B. Foresman, in: E. Frisch (Ed.), Exploring chemistry with Electronic Structure methods: A Guide to Using Gaussian, Pittsburg, PA, 1996.
12. J.J. Nie, D.J. Xu, J. Chinese, Struct. Chem. 21 (2002) 165-167.
13. H.S. Chen, Z.M. Li. X.P.Yang, H.G. Wang, X.K. Yao, Chin. J. Struct. Chem. 19 (2000) 317-325.
14. M. Kaur, Y.S. Mary, C.Y. Panicker, H.T. Varghese, H.S. Yathirajan, K. Byrappa, C. Van Alsenoy, Spectrochim. Acta A 120 (2014) 445-455.
15. A. Cravino, H. Neugebauer, S. Luzzati, M. Catellani, N.S. Sariciftci. J. Phys. Chem. 105B (2001) 46-52.
16. R.M. Silverstein, G.C. Bassler, T.C. Morril, Spectrometric identification of Organic Compounds, fifth ed., John Wiley and Sons, Inc., Singapore, 1991.
17. S. Genc, N. Dege, A. Cetin, A. Cansiz, M. Sekerci, M. Dincer, Acta Cryst. E60 (2004) 1340-1340.
18. F.R. Dollish, W.G. Fateley, F.F. Benteley, Characteristic Raman Frequencies of Organic Compounds, Wiley, New York (1997).
19. G. Varasanyi, Vibrational Spectra of Benzene Derivatives, Academic Press, New York, 1969.
20. M. Pagannone, B. Formari, G. Mattel, Spectrochim. Acta A 43 (1986) 621-625.
21. N.P.G. Roeges, A Guide to the Complete Interpretation of IR Spectra of Organic compounds, Wiley, New York, 1994.
22. R. Ustabas, N. Suleymanoglu, H. Tanak, Y.B. Alpaslan, Y. Unver, K. Sancak, J. Mol. Struct. 984 (2010) 137-145.
23. A. Siweek, M. Wujec, I. Wawrzycka-Gorczyca, M. Dobosz, P. Paneth, Heteroat. Chem. 19 (2008) 337-344.
24. Y. Unver, K. Sancak, H. Tanak, D. Degirmencioglu, E. Dugdu, M. Er. S. Isik. J. Mol. Struct. 936 (2009) 46-55.
25. N. Suleymanoglu, R. Ustabas, Y.B. Alpaslan, Y. Unver, M. Turan, K. Sancak, J. Mol. Struct. 989 (2011) 101-108.
26. D. Lin-vien, N.B. Colthup, W.G. Fately, J.G. Grasselli, The Handbook of Infrared and Raman Characteristic frequencies of Organic Molecules, Academic Press Limited, London, 1991.
27. C.Y. Panicker, M.R. Anoop, P.S. Binil, Y.S. Mary, H.T. Varghese, T.K. Manojkumar, Int. J. Ind. Chem. 2 (2011) 33-44.
28. P.S. Binil, M.R. Anoop, Y.S. Mary, H.T. Varghese, C.Y. Panicker, S. Suma, M.R. Sudarsanakumar, Int. J. Ind. Chem. 2 (2011) 1-11.
29. N.A. Mangalam, C.Y. Panicker, S.R. Sheeja, M.R.P. Kurup, Y.S. Mary, K. Raju, H.T. Varghese, V.M. Nair, Int. J. Ind. Chem. 1 (2010) 17-28.
30. G. Socrates, Infrared Characteristic Group Frequencies, John Wiley and Sons, New York, 1981.
31. K. Nakanishi, Infrared Absorption Spectroscopy Practical, Holden-Day, San Francisco, 1962.
32. Y.R. Sharma, Elementary organic spectroscopy principles and chemical applications, S. Chand and Company Ltd., New Delhi, (1994).
33. N.B. Colthup, I.H. Daly, S.E. Wiberly, Introduction to Infrared and Raman Spectroscopy, third ed., Academic Press, Boston, 1990.

34. C. Crak, Y. Sert, F. Ucun, Effect of intermolecular hydrogen bonding, vibrational analysis and molecular structure of 4-chlorobenzothioamide, Spectrochim. Acta A 113 (2013) 130-136.
35. V. Arjunan, R. Santhanam, S. Sakiladevi, M.K. Marchewka, S. Mohan, Synthesis and characterization of an anticoagulant 4-hydroxy-1-thiocoumarin by FTIR, FT-Raman, NMR, DFT, NBO and HOMO-LUMO analysis, J. Mol. Struct. 1037 (2013) 305-316.
36. G. Socrates, Infrared and Raman Characteristic Group Frequencies, Tables and Charts, third ed., John Wiley, Chichester, 2001.
37. A. Coruh, F. Yilmaz, B. Sengez, M. Kurt, M. Cinar, M. Karabacak, Synthesis, molecular conformation, vibrational, electronic transition and chemical shift assignments of 4-(thiophene-3-ylmethoxy) phthalonitrile: A combined experimental and theoretical analysis, Struct. Chem. 22 (2011) 45-56.
38. M. Karabacak, S. Bilgili, T. Mavis, M. Eskici, A. Atac, Molecular structure, spectroscopic characterization (FT-IR, FT-Raman, UV and NMR), HOMO and LUMO analysis of 3-ethynylthiophene with DFT quantum chemical calculations, Spectrochim. Acta A 115 (2013) 709e718.
39. I. Fleming, Frontier Orbitals and Organic Chemical Reactions, Wiley-Blackwell, New York, 1976.
40. I. Fleming, Frontier Orbitals and Organic Chemical Reactions, John Wiley & Sons, New York, 1976.
41. J. Aihara, J. Phys. Chem. 103A (1999) 7487.
42. C.G. Zhan, J.A. Nochols, D.A. Dixon, J. Phys. Chem. 107A (2003) 4184.
43. R.G. Parr, L.V. Szentpaly, S. Liu, J. Am. Chem. Soc. 121 (1999) 1922.
44. M. Elango , R. Parthasarathi , G. Karthik Narayanan , A. MD. Sabeelullah , U. Sarkar, N. S. Venkatasubramaniyan , V. Subramanian and P. K. Chattaraj, J. Chem. Sci., Vol. 117, No. 1, (2005), pp. 61–65.
45. F.J. Luque, J.M. Lopez, M. Orosco, Theor. Chem. Acc. 103 (2000) 343.
46. H.Kobinyi, G. Folkers, Y.C. Martin, 3D QSAR in Drug Design, Recent Advances, vol. 3, Kluwer Academic Publishers, 1998.
47. M. Szafran, A. Komasa, E.D. Adamaska, J. Mol. Struct. Theochem. 827 (2007) 101-107.
48. L. Rajith, A.K. Jissy, K.G. Kumar, A. Datta, J. Phys. Chem. C115 (2011) (1864) 21858-21864.
49. A.E. Reed, L.A. Curtis, F.A. Weinhold, Chem. Rev. 88 (1988) 899-926.
50. P.V. Kolinzky, Opt. Eng. 31 (1992) 1676-1684.
51. D.F. Eaton, Science 253 (1991) 281-287.
52. N. Sundaraganesan, E. Kavitha, S. Sebastian, J.P. Cornard, M. Martel, Spectrochemica Acta A, 74 (2009) 788-797.
53. H. Alyar, Z. Kantarci, M. Bahat, E. Kasap. J. Mol. Struc. 834-836 (2007) 516-520.
54. K.I. Jayalakshmi, B.T. Gowda, Z. Naturforsch. 59 (2004) 491-500.
55. B.T. Gowda, S. Foro, H. Fuess, Acta Cryst. 63 (2007) 2338.
56. E. Pretsch, P. Buhlmann, C. Affolter Struct, Determination of Organic Compounds, Springer-Verlag, Berlin Heidelberg New York, 2000.
57. A. R. Choudhury, T.N. Guru Row, Acta Cryst. 60 (2004) 1595-1597.
58. Z.Liu, Y. Au, M. Tan, H. Zhu, Acta Cryst. 60 (2004) 1310-1311.
59. R.G. Parr, W. Yang, Functional Theory of Atoms and Molecules, Oxford University Press, New York, (1989).
60. P.W. Ayers, R.G. Parr, J. Am. Chem. Soc. 122 (2000) 2010-2018.
61. R. G. Parr, W.J. Yang, Am. Chem. Soc. 106 (1984) 511-513.
62. P.K. Chattaraj, B. Maiti, U. Sarkar, J. Phys. Chem, A 107 (2003) 4973-4975.
63. C. Morell, A. Grand, A. Toro-Labbe, J. Phys. Chem. A 109 (2005) 205-212.
64. R.S. Mulliken, J. Chem. Phys. 23 (1955) 1833-1840.
65. M.C. Gupta, Atomic and Molecular Spectroscopy, New Age International Private Limited Publishers, New Delhi, (2001).